Copyright Warning & Restrictions

The copyright law of the United States (Title 17, United States Code) governs the making of photocopies or other reproductions of copyrighted material.

Under certain conditions specified in the law, libraries and archives are authorized to furnish a photocopy or other reproduction. One of these specified conditions is that the photocopy or reproduction is not to be "used for any purpose other than private study, scholarship, or research." If a, user makes a request for, or later uses, a photocopy or reproduction for purposes in excess of "fair use" that user may be liable for copyright infringement,

This institution reserves the right to refuse to accept a copying order if, in its judgment, fulfillment of the order would involve violation of copyright law.

Please Note: The author retains the copyright while the New Jersey Institute of Technology reserves the right to distribute this thesis or dissertation

Printing note: If you do not wish to print this page, then select "Pages from: first page # to: last page #" on the print dialog screen

ABSTRACT

EXPERIMENTAL DETERMINATION OF THE MIXING REQUIREMENTS FOR SOLID SUSPENSION IN PHARMACEUTICAL STIRRED TANK REACTORS

by
Anqi Zhou

Glass and glass-lined, stirred-tank reactors are of significant importance in the pharmaceutical and related industries. Because of fabrication issues, a retreat blade impeller (RBI) with a low impeller clearance off the tank bottom is commonly used in glass-lined reactors, typically combined with a single baffle (providing only partial baffling conditions) mounted from the top of the reactor. In addition, these reactors are often provided with a torispherical bottom. Other configurations are also used, including full baffling or no baffles at all, hemispherical bottoms, and different impeller types. Despite their common use, some of the most important mixing characteristics of this type of reactor have not been fully studied, such as the minimum impeller agitation speed, N_{js}, to just suspend finely divided solids.

In this work, N_{js} was experimentally obtained for a number of different pharmaceutically-relevant agitation systems including vessels with different types of bottoms (torispherical or hemispherical), impeller types (RBI, disk turbine, 4-blade and 6-blade pitched-blade turbine), baffling conditions (fully baffled, partially baffled, and unbaffled tanks), impeller clearance off the tank bottom, and solid particle size. The power dissipated by the impeller was also measured.

A novel experimental approach to determine N_{js} was developed here. This approach consists of experimentally measuring the size of the circular region of the tank bottom covered by the solids at increasing values of the agitation speed, N, plotting N vs.

the size of this region (expressed as either the region's diameter D_S or its area A_S), and linearly regressing the data to obtain N_{js} as the limit of the N value for D_S or A_S going to zero. The N_{js} results obtained with the new approach were compared with those obtained using the traditional Zwietering's approach, visually requiring that the solids do not rest on the tank bottom for more than 1-2 seconds. Excellent agreement was found between the results obtained using the novel approach and those obtained using Zwietering's method. The novel method proposed here completely eliminates the observer's bias from the experimental determination of N_{js}.

The results obtained here show that N_{js} is a strong function of most of the variables listed above, and especially the baffling type.

EXPERIMENTAL DETERMINATION OF THE MIXING REQUIREMENTS FOR SOLID SUSPENSION IN PHARMACEUTICAL STIRRED TANK REACTORS

by
Anqi Zhou

A Thesis
Submitted to the Faculty of
New Jersey Institute of Technology
in Partial Fulfillment of the Requirements for the Degree of
Master of Science in Pharmaceutical Engineering

Otto H. York Department of Chemical, Biological and Pharmaceutical Engineering

May 2014

APPROVAL PAGE

EXPERIMENTAL DETERMINATION OF THE MIXING REQUIREMENTS FOR SOLID SUSPENSION IN PHARMACEUTICAL STIRRED TANK REACTORS

Anqi Zhou

Dr. Piero M. Armenante, Thesis Advisor Date
Distinguished Professor of Chemical, Biological and Pharmaceutical Engineering, NJIT

Dr. Laurent Simon, Committee Member Date
Associate Professor of Chemical, Biological and Pharmaceutical Engineering, NJIT

Dr. Xianqin Wang, Committee Member Date
Associate Professor of Chemical, Biological and Pharmaceutical Engineering, NJIT

BIOGRAPHICAL SKETCH

Author: Anqi Zhou

Degree: Master of Science

Date: May 2014

Undergraduate and Graduate Education:

Master of Science in Pharmaceutical Engineering,
New Jersey Institute of Technology, Newark, NJ, 2014

Bachelor of Engineering in Bioengineering,
Dalian Nationalities University, Dalian, P. R. China, 2012

Major: Pharmaceutical Engineering

To My Family

ACKNOWLEDGMENT

I owe my gratitude to all those people who have made this thesis possible and because of whom my graduate experience has been one that I will cherish forever.

My deepest gratitude is to my advisor, Dr. Piero M. Armenante. I have been amazingly fortunate to have an advisor who gave me the freedom to explore on my own, and at the same time the guidance to recover when my steps faltered. Dr. Armenante taught me how to question thoughts and express ideas. His patience and support helped me overcome many crisis situations and finish this thesis.

I would like to acknowledge Dr. Laurent Simon and Dr. Xianqin Wang for their patience in reviewing the thesis, for their recommendations and everything

Finally, I would like to express my deepest gratitude towards Bing Wang who helped me a lot during my thesis study.

TABLE OF CONTENTS

TABLE OF CONTENTS
(Continued)

Chapter **Page**

LIST OF TABLES

Table **Page**

LIST OF FIGURES

LIST OF FIGURES
(Continued)

NOMENCLATURE

D	Impeller diameter (mm)
T	Tank diameter (mm)
H	Liquid height (mm)
C_b	Bottom clearance (mm)
N	Rotational speed (rpm)
N_{js}	Minimum agitation speed for solid suspension
P	Dissipation power (watt)
τ	Torque (Nm)

CHAPTER 1

INTRODUCTION

1.1 Background Introduction

Glass-lined reactors are commonly used in the chemical and pharmaceutical industries. Glass lining provides corrosion resistance, ease of cleaning, and reduced product contamination. A typical glass-lined reactor is equipped with a single retreat-blade impeller (RBI) close to the tank bottom and a single baffle. Baffles are long flat plates that attach to the side of the tank to prevent swirling and promote top to bottom movement. A standard baffling configuration in most mixing tanks consists of four vertical having width equal to 8% to 10% (T/12 to T/10) of the tank diameter. Without baffling or with insufficient baffling, the fluid moves in a swirling motion in the tank creating a central vortex, and mixing is insufficient (Myers and Reeder, 2002). Installing baffles eliminates such swirling motion by breaking a vortex and ultimately improving the mixing process. Solid suspension and dispersion in a liquid is an important operation carried out in such mixing systems. The primary objective of solid-liquid mixing is to create and maintain solid-liquid slurry, and to promote and enhance the rate of mass transfer between the solid-liquid phases. Solid suspension is very common during API manufacturing (e.g., crystals).

In agitated vessels, the degree of solid suspension is generally classified into three levels: on-bottom motion, complete off-bottom suspension, and uniform suspension (Paul et al., 2004). For many applications, it is often important just to provide enough agitation to completely suspend the solids off the tank bottom. Below this off-bottom particle suspension state, the total solid-liquid interfacial surface area is not completely or

efficiently utilized. Therefore, it is important to be able to determine the impeller agitation speed N_{js}, at which the just suspended state is achieved by the particles (Armenante and Uehara-Nagamine 1998). Although N_{js} has been obtained for a number of mixing systems, very little information is available in the literature for the solid suspension in the system most commonly used in pharmaceutical industry, i.e., a torispherical bottomed tank provided with a Pfaudler-type of impeller (i.e., a three-blade, retreat-blade impeller) and a single baffle.

1.2 Objectives of This Work

The typical method to measure experimentally N_{js} is that of Zwietering's (1958). Accordingly, N_{js} is obtained by visually inspecting the tank bottom and visually determining the impeller agitation speed at which the solids are observed to rest on the tank bottom for no more than 1-2 seconds before being swept away. Although this method is quite reliable, there is clearly the need to develop a method that is not observer-based. Therefore, the first objective of this work was to experimentally develop a new method to determine the minimum agitation speed, N_{js}, for just solid suspension that did not rely just on the observed assessment of the just-suspended solid state.

This objective was pursued and eventually achieved by using a novel approach based on the measurement of the of the size of the circular region of the tank bottom covered by the solids at increasing values of the agitation speed, N, plotting N vs. the size of this region (expressed either as the region's diameter D_S or region's area A_S), and then linearly regressing the data to obtain N_{js} as the limit of the N value for D_S or A_S going to zero.

Once this approach was validated against the conventional visual approach to N_{js} determination, a second objective was pursued, i.e., the determination of N_{js} for a variety of

mixing systems of relevance to the pharmaceutical industry, and especially the glass-lined type of tank with a torispherical bottom agitated with a retreat-blade impeller (RBI) commonly used for chemical synthesis.

The configuration of the system used here is based on the previous work of Nonjaros Chomcharn and Dilanji Bhagya Wijayasekara who completed their thesis in this lab. Additionally to prove the novel method approach can be used in general tank mixing system, different tank systems (torispherical-bottomed tank, hemispherical-bottomed tank), different impeller types (retreat-blade curved impeller (RBI), 4-blade and 6-blade pitched-blade turbine (4-PBT and 6-PBT), disk turbine (DT)) and different baffling configurations (fully baffled, partially baffled and unbaffled) must consider.

CHAPTER 2

EXPERIMENTAL APPARATUS, MATERIALS AND METHODS

2.1 Apparatus

2.1.1 Torispherical-Bottom Mixing Vessel and Impellers

A scaled-down model of a commercial (DeDietrich), torispherical-bottomed (dish-bottomed) reactor, similar to the type of glass-lined reactors frequently utilized in the pharmaceutical industry was used. This tank was commissioned, and paid for, by Eli Lilly (thanks to Dr. Billy Allen, Eli Lilly, Indianapolis, IN). BHR Group in the UK (with Dr. David Brown's assistant) completed the fabrication of this tank. It is made of a thin (0.5 mm) fluorinated ethylene propylene co-polymer (FEP) semi-rigid film having a refractive index of 1.338, which is very close to that of water (1.333) in order to minimize curvature effects during observation and image processing steps. The basic dimensions of this tank, shown in Figure 2.1 (a), were as follows:

- Internal diameter (T): 450 mm
- Overall height: 540 mm
- Height of dish bottom: 155 mm
- Height of cylindrical section: 385 mm

The tank had a rigid collar and lip at its top, which allowed the tank to be suspended in a larger 'host' square tank, as shown in Figure 2.1(a). During the experiment, the mixing tank was placed in the host Plexiglas square tank filled with water in order to minimize the optical distortion introduced by the curvature of the cylindrical mixing tank. The mixing

tank was filled with water so that the liquid level, H, was equal to the tank diameter (H/T = 1), corresponding to a liquid volume, V, of 60.488 liters.

Circles and radii were drawn on the tank bottom using a black mark pen in order to measure the portion of the tank bottom covered by solids during an experiment, as shown in Figure 2.1(b).

Experiments in this system were conducted under three baffling configurations, i.e., with unbaffled, partially baffled, and fully baffled tanks. For the partially baffled system, a single beaver-tail baffle (Figure 2.2) was placed midway between the tank wall and the central impeller shaft (baffle distance from the wall: 75 mm). In the fully baffled system, four vertical baffles were mounted and fixed from the top of the tank. Each of the baffles was made of two pieces vertical rectangular metal plates (width 25 mm and 19.1mm) mounted from the top. The total width of each baffle was 44.1 mm.

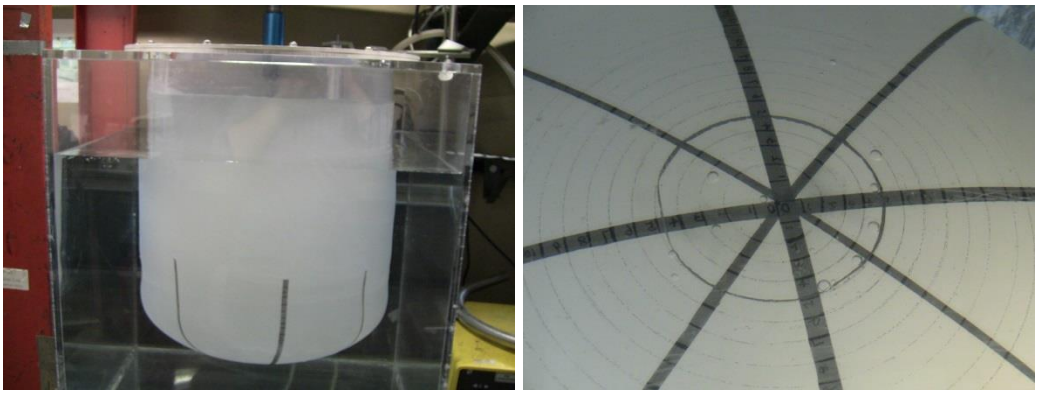

(a) (b)

Figure 2.1 (a) Torispherical-bottomed glass-lined tank system (b) Bottom view of the tank with equally spaced circles drawn on its bottom.

Figure 2.2 Single Beaver-tail Baffle.

Two types of impellers were used in this system, as shown in Figures 2.3(a) and (b). Most experiments were conducted with a scaled-down version (based on that of the De Dietrich Company) of a single retreat-blade, three-blade curved impeller (RBI), used with glass-lined vessels in the pharmaceutical industry (Figure 2.3(a)). The following are the impeller dimensions measured with a caliper: impeller diameter (D) = 203 mm; the radius of curvature of the blades = 92.08 mm; height of the blade = 25.4 mm; thickness of the blade = 12.7 mm; and an impeller diameter-to-tank diameter ratio, D/T, of 0.451. The impeller was kindly donated by Dr. San Kiang of Bristol-Myers Squibb, New Brunswick, NJ. The other impeller was a typical four-blade, 45^0 pitch-blade turbine (4-PBT; Figure 2.3(b)). The dimensions of the 4-PBT were as follows: impeller diameter D = 190.6 mm; blade length = 75.7 mm; blade width = 38.4 mm; and blade thickness = 3.2 mm. The impeller clearance was varied depending on the experiments.

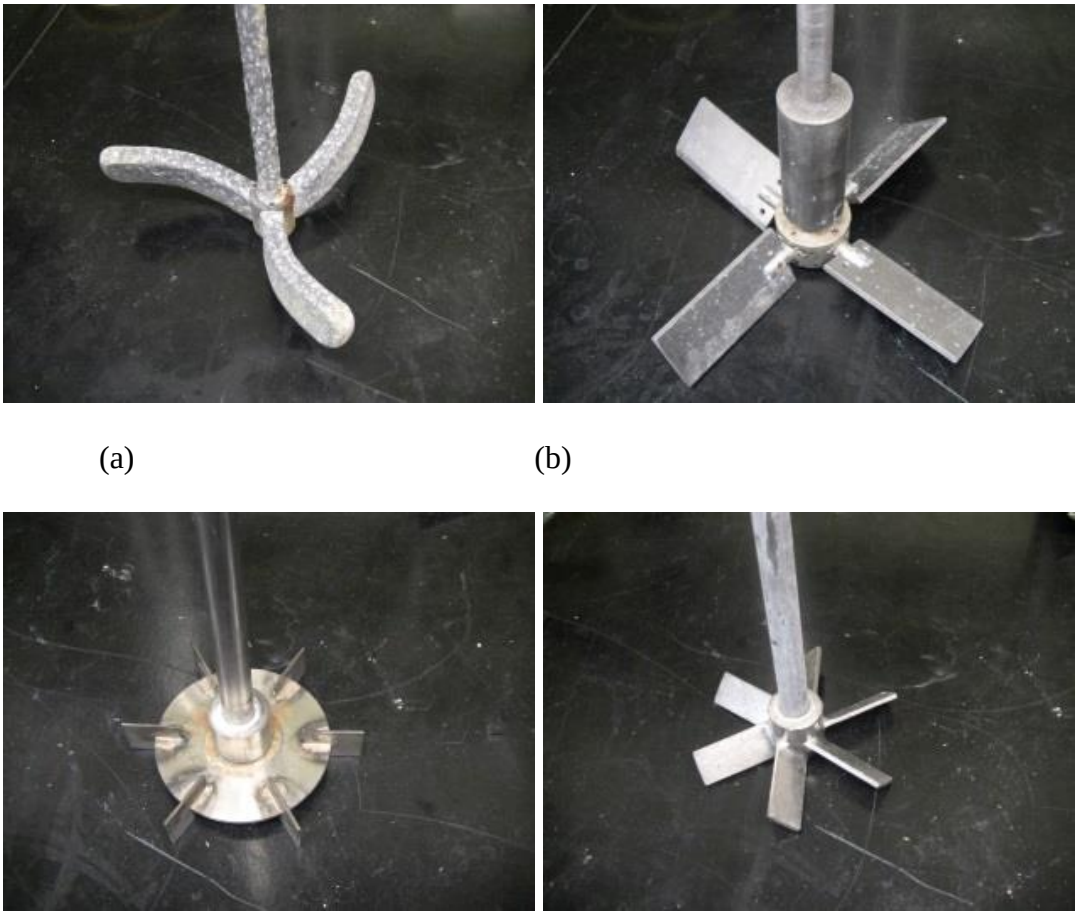

(a) (b)

(c) (d)

Figure 2.3 Impellers used in this work: (a) RBI impeller (b) 4-blade PBT (c) DT; and (d) 6-PBT. Impellers (a) and (b) were used in the torispherical-bottom mixing system and impellers (c) and (d) were used in the hemispherical-bottom mixing system.

2.1.2 Hemispherical-Bottom Mixing Vessel and Impellers

An open glass cylindrical tank with a hemispherical bottom was also used. The total tank height for this tank was 530 mm and its internal diameter was 300 mm. The bottom section of the glass tank was 100 mm and the cylindrical section was and 430 mm, although the tank was filled with water so that the liquid level, H, was equal to the tank diameter (H/T = 1), corresponding to a liquid volume, V, of 17.1 liters. The glass tank was supported by a square bracket (kindly made by Mr. Shawn Yetman) and placed in the host Plexiglas

square tank in order to minimize the optical distortion introduced by the curvature of the cylindrical mixing tank. This tank was operated under two baffling conditions, i.e., either unbaffled of fully baffled. For the fully baffled tank, the baffles were set up similarly to the torispherical system, but the baffle width was 25 mm. Two types of impellers were used in this system, i.e., a six-blade, 45º degree pitched-blade turbine (6-PBT) and a 6-blade disk turbine (DT), as shown in Figures 2.3(c) and (d). The dimensions of the impellers are as follows: for the DT, impeller diameter D = 102.5 mm, blade height: 20.3 mm, blade length= 20.4 mm, blade thickness = 1.7 mm; for the 6-PBT: D = 102.5 mm, blade width: 17.5 mm, blade length= 20.4 mm, blade thickness = 1.7 mm.

2.1.3 Agitation System and Data Acquisition

The selected impeller were attached to a central located shaft (diameter 12.52 mm) inside the tank, rotated by a 0.25 HP motor (Chemglass, Model CG-2033-11) controlled by an external controller (Chemglass, Model CG-2033-31), as shown in Figure 2.4.

A data acquisition system was used to measure the agitation speed, the torque applied to the impeller, and the power dissipated by the impeller. The torque (Γ) applied to the impeller by the motor was experimentally measured using a strain gage-based rotary torque transducer (Model, T6-5-Dual Range, Interface, Inc. Scottsdale, AZ) mounted between the motor and the impeller. The transducer was connected to the Interface series 9850 Multi-Channel Load Cell Indicator. The transducer can measure the torque in two different scales, i.e., 0-0.5 Nm and 0-5 Nm. The same instrument could also measure the agitation speed, N, and internally calculate the instantaneous power delivered, P, by the shaft according to (Brown et al., 2004):

$$P = 2\pi N \Gamma$$

The indicator utilized the M700 software to interface with a computer, which was used for data acquisition and processing.

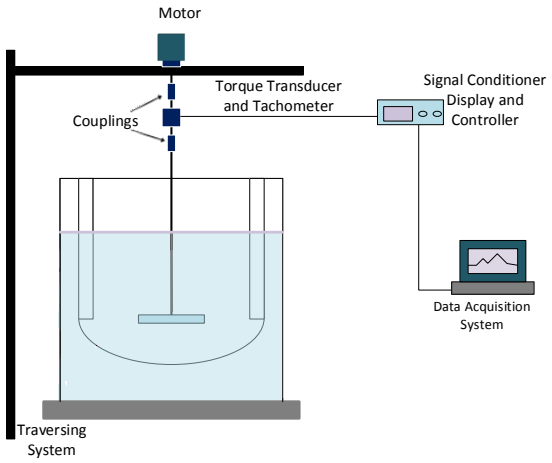

Figure 2.4 Schematic of experimental set-up of agitation system.

2.2 Materials

Tap water at room temperature was used as the liquid in all experiment. The liquid height was equal to the tank diameter in all cases. Glass beads having average of diameters of 150 µm and 200 µm were used as the disperse phase. Prior to their use, prescreened glass beads were sieved. Four US standard screens of mesh size 40, 60, 80 and 100 were selected. 30 g of glass beads were processed at a time, by placing them in the top screen with the smallest mesh size, and shaking them for five minutes. The particles retained on the size 100 mesh screen (with an average diameter size of 150 µm) and size 80 mesh screen (with an average diameter size of 200 µm) were collected separately and used in the experiments. In each experiment, the solid fraction of solids was equal to 0.5% of the liquid weight (g/g), corresponding to 302 g in the in torispherical tank, and 85.5 g in hemispherical tank, respectively, as measured by an electronic scale.

2.3 Experimental Method and Approach to N_{js} Determination

Before each experiment, the selected mixing tank was inserted in the square tank and the whole assembly was placed on a heavy-duty lift platform. This assembly was positioned under the impeller so that the impeller was centered in the mixing tank. The mixing tank and the square tank were then filled with tap water, up to 450 mm for glass-lined tank and 300 mm for the glass system, so that H/T = 1 in all cases. The impeller off-bottom clearance, C_b, measured from the bottom of the impeller to the bottom of the tank along the tank centerline, was set to the required value by moving the whole tank assembly vertically. The solid particles were then added and a mirror was placed at a 45^0 angle under the tank so that the bottom of the mixing tank could be clearly seen, a light illuminating the bottom portion of the vessel was turned one, and a video camera (VIXIA HF200, Canon) was used to record the solid distribution on the vessel bottom.

An interesting phenomenon was observed in the torispherical-bottom tank. This tank was made of a thin FEP semi-rigid film and could be easily deformed. Therefore, this tank was placed in the square tank, which was filled with water to a level similar to the liquid level inside the FEP tank to minimize mechanical stresses on the FEP wall. However, at higher agitation speeds it was noticed that the bottom portion of the FEP vessel just under the impeller would deform slightly and lift up in response to the low pressure region generated just below the rotating impeller. In order to compensate, the water level in the square tank was lowered until no such a deformation of the tank bottom occurred.

The approach used here to determine N_{js} was derived from the "steady cone radius method" (SCRM) developed by Brucato et al. (2010). These authors studied solid

suspension in top-covered unbaffled tanks by taking images of the vessel bottom at different N values using low shutter speeds (large image capture times) to determine which portion of the solids cone was rotating and which was not. They obtained N_{js} by determining the N value at which the inner stationary solids portion would vanish.

In this work, a typical experiment consisted of setting the agitation speed at a given value N, video recording the vessel bottom to determine the region of the tank bottom covered with solids once a dynamic equilibrium had been reached, and repeating this procedure at increasing values of the impeller agitation speed. Since the tank bottom had been marked with circles and radii emanating from the vessel bottom center, both the diameter D_S of the area covered by solids at a given N and the corresponding area A_S could be recorded and measured. Typically, the solids covered on a circular area, although non-circular areas were also observed, in which case the average values of D_S and A_S were recorded. In a typical experimental run in the torispherical-bottomed tank system, N values were typically recorded at D_S values equal to 10 cm, 9 cm, 8 cm, 7 cm, 6 cm, and 5 cm. In the hemispherical tank, N measurements were typically taken at DS values equal to 8 cm, 6 cm, 4 cm, 2 cm. Plots of N vs. D_S and N vs A_S were then constructed, and linear regression lines were obtained to find the predicted extrapolated values of N when $D_S \rightarrow 0$ as well as when $A_S \rightarrow 0$. These values were taken as the expected N_{js} values based on these two approaches, and were labeled respectively as $N_{js\text{-}Ds\text{-}Method}$ and $N_{js\text{-}As\text{-}Method}$. Examples of this method are presented in Figure 3.1. In addition, the visual value of N_{js} ($N_{js\text{-}Visual}$) was obtained using the Zweitering's criterion (Zwietering, 1958), defined as the agitation speed at which no particles were visually observed to be at rest on the tank bottom for more than one to two seconds. In general, $N_{js\text{-}Ds\text{-}Method}$ was found to agree well with $N_{js\text{-}Visual}$ for

unbaffled systems whereas $N_{js\text{-}As\text{-}Method}$ was found to agree with $N_{js\text{-}Visual}$ for fully baffled and partially baffled systems, as further discussed in the Results section.

All experiments were repeated in triplicates. The power dissipation at each agitation speed was also recorded. Experiments were conducted in different vessels, using different impellers, impeller clearances, baffling conditions, and particles size, as summarized in Table 2.1.

Table 2.1 Summary of Experimental Conditions and Variable Ranges Tested in This Work.

System Variable	Torispherical-Bottomed Tank	Hemispherical-Bottomed Tank
Impeller Type	RBI, 4-PBT	DT, 6-PBT
Baffling Conditions	UB, PB, FB	UB, FB
C_b/T	0.333, 0.267, 0.2, 0.133, 0.089	0.333, 0.267, 0.2, 0.133, 0.089
Particle Size	150 μm (for RBI only); 200 μm	200 μm

CHAPTER 3

RESULTS AND DISCUSSION

3.1Results of Solid Suspension Experiment

3.1.1 Comparison of the N_{js} Values Obtained with the Proposed Methods with Those Obtained with the Conventional *Zwietering's* Approach

In this section, the results of the experiments aimed at validating the proposed method are presented and compared with results obtained the conventional *Zwietering's* approach.

According to the procedure developed for the proposed method, the values of D_S of A_S were obtained at increasing values of the agitation speed, N. For each experimental configuration at least four measurements of N vs. D_S and N vs. A_S were taken. $N_{js\text{-}Visual}$ was also determined. All experiments were conducted in triplicate. Figures 3.1-3.5 show the N-vs.-D_S and N-vs.-A_S plots for different cases and the resulting N_{js} values.

The values of N_{js} were firstly experimentally obtained in torispherical-bottomed tank equipped with the three-blade retreat-blade curved impeller (RBI) with two particle sizes, 150 µm and 200 µm. The results for are shown in Figure 3.1 for 150 µm particles. The first observation from this figure is that the experimental points align themselves on straight lines (R=0.992). It is therefore possible to regress the lines and predict the value of N_{js} at the intersection of each line with the y-axis, thus identifying the values of $N_{js\text{-}As\text{-}Method}$ and $N_{js\text{-}Ds\text{-}Method}$. For the fully baffled systems, Figure 3.1 (a) and Figure (b) show that $N_{js\text{-}Visual}$ is 246.44 rpm, $N_{js\text{-}As\text{-}Method}$ is 244.72, N_{js} by $N_{js\text{-}Ds\text{-}Method}$ is 281.01 rpm, i.e., that the $N_{js\text{-}As\text{-}Method}$ is in excellent agreement with the visually determines value of N_{js}. However, the difference between $N_{js\text{-}Visual}$ and $N_{js\text{-}Ds\text{-}Method}$ is significant. This implies that, at least for this case, the A_S method is a valid alternative to the conventional method to determine N_{js}.

For the partially baffled system shown in Figure 3.1 (c) and Figure 3.1(d), visual observation resulted in an N_{js} value of 166.96 rpm, which is close to $N_{js\text{-}As\text{-}Method}$ (161.04 rpm) whereas $N_{js\text{-}Ds\text{-}Method}$ was 192.92 rpm. However, for the unbaffled case shown in Figure 3.1 (e) and Figure 3.1 (f) visual observation resulted in $N_{js\text{-}Visual}$ equal to 178.24 rpm which is very similar to N_{js} measured by $N_{js\text{-}Ds\text{-}Method}$ (182.74 rpm) but different from the $N_{js\text{-}As\text{-}Method}$ (145.11 rpm), unlike the fully baffled and partially baffled systems.

The results for similar systems but with larger particles (d_p = 200 μm) are shown in Figure 3.2. As before, the $N_{js\text{-}As\text{-}Method}$ was in excellent agreement with $N_{js\text{-}Vsual}$ in the fully baffled system and partially baffled system, whereas $N_{js\text{-}Ds\text{-}Method}$ agreed with the visual measurement of N_{js} in the unbaffled system. This means $N_{js\text{-}As\text{-}method}$ and $N_{js\text{-}Ds\text{-}method}$ can be applied to determination of N_{js} depending on the baffling configuration at least in torispherical-bottomed tank with retreat-blade curved impeller.

To determine if the novel method can be used in general in torispherical-bottomed tanks, a four-blade pitched-blade turbine (4-PBT) was used. Similar results were obtained as shown in Figure 3.3. In the fully baffled system, the value of N_{js} visual observation is 135.72 rpm and the N_{js} by As-method is 132 rpm. In the partially baffled system, the value of N_{js} by visual observation is 141.74 rpm compared to 138.96 rpm by As-method. In the unbaffled configuration, the visually observed N_{js} (151.32 rpm) agreed with the N_{js} (152.79 rpm) obtained by Ds-method.

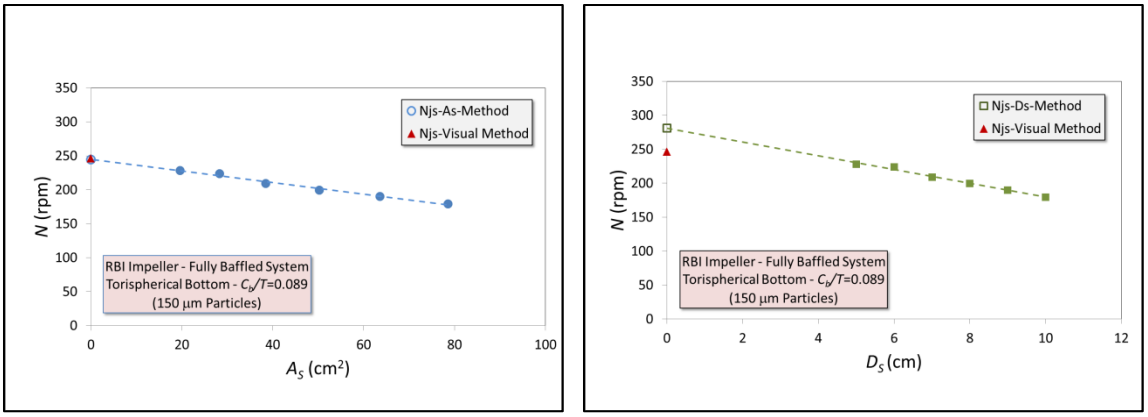

(a)

(b)

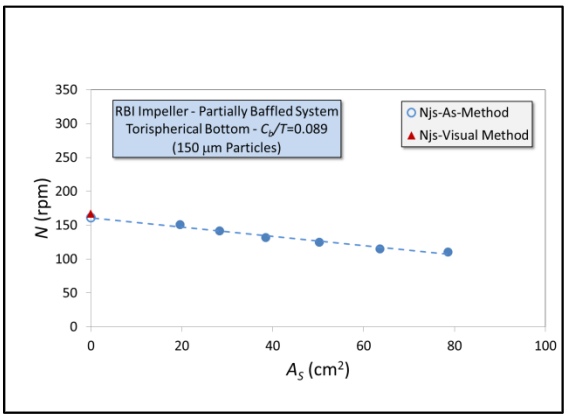

(c)

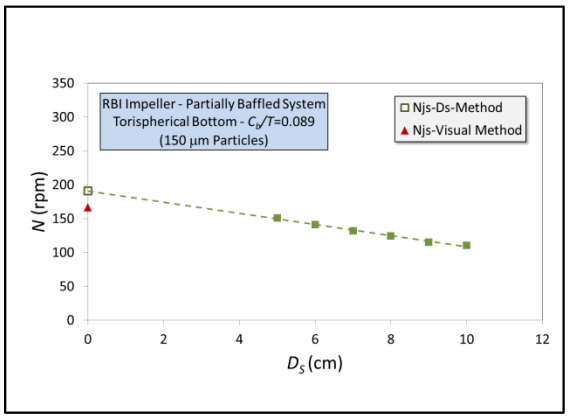

(d)

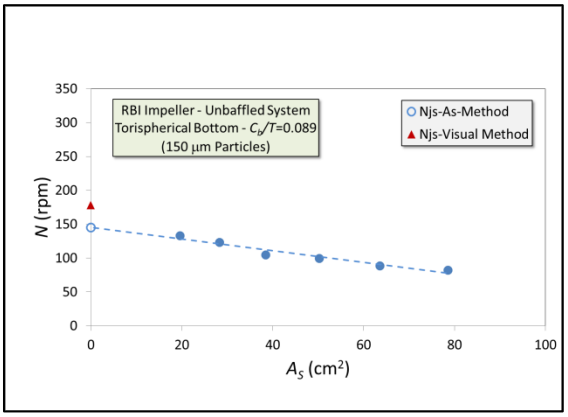

(e)

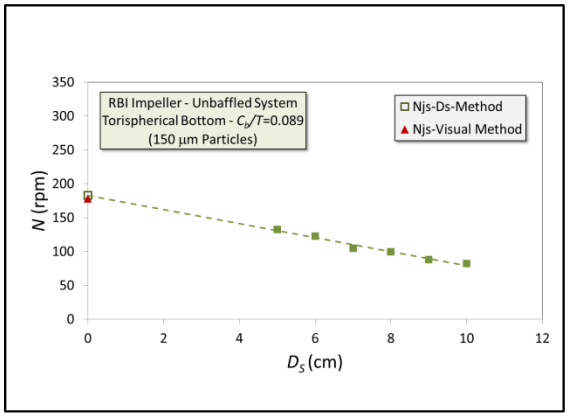

(f)

Figure 3.1 N_{js} measured the torispherical-bottomed tank with the RBI using for 150 µm particles: (a) $N_{js\text{-}As\text{-}Method}$ in fully baffled system (b) $N_{js\text{-}Ds\text{-}Method}$ in fully baffled system (c) $N_{js\text{-}As\text{-}Method}$ in partially baffled system (d) $N_{js\text{-}Ds\text{-}Method}$ in partially baffled system (e) $N_{js\text{-}As\text{-}Method}$ in unbaffled system (f) $N_{js\text{-}Ds\text{-}Method}$ in unbaffled system.

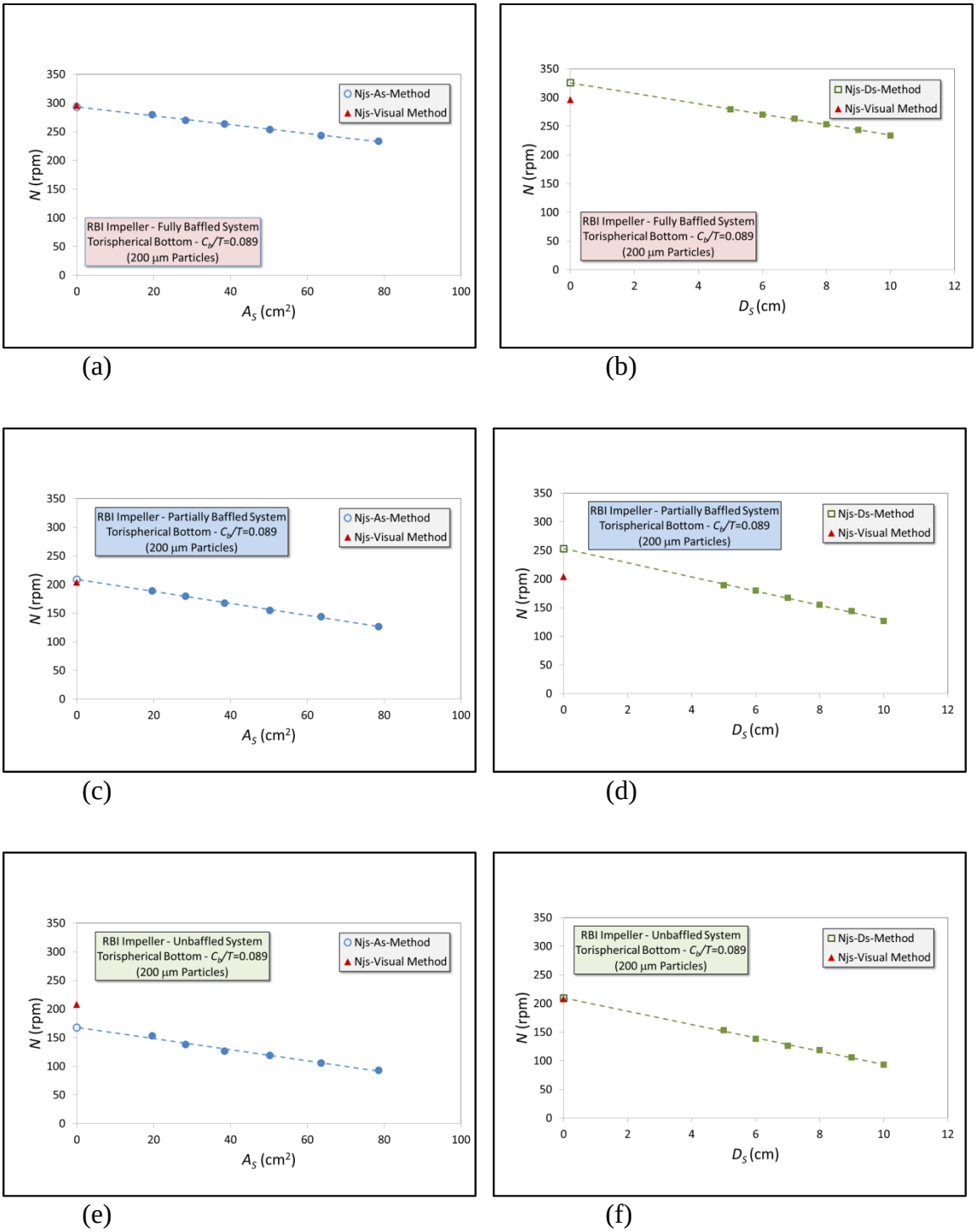

Figure 3.2 N_{js} measured in the torispherical-bottomed tank with the RBI using for 200 µm particles: (a) $N_{js\text{-}As\text{-}Method}$ in fully baffled system (b) $N_{js\text{-}Ds\text{-}Method}$ in fully baffled system (c) $N_{js\text{-}As\text{-}Method}$ in partially baffled system (d) $N_{js\text{-}Ds\text{-}Method}$ in partially baffled system (e) $N_{js\text{-}As\text{-}Method}$ in unbaffled system (f) $N_{js\text{-}Ds\text{-}Method}$ in unbaffled system.

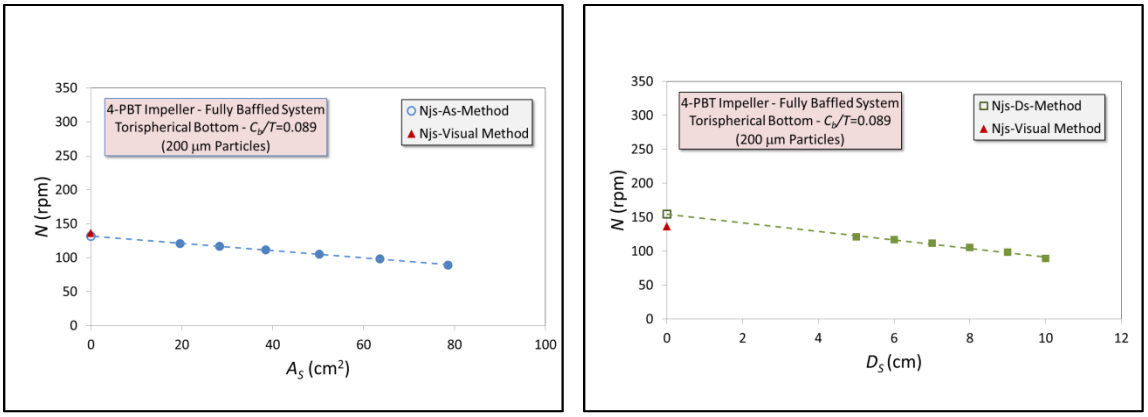

(a)

(b)

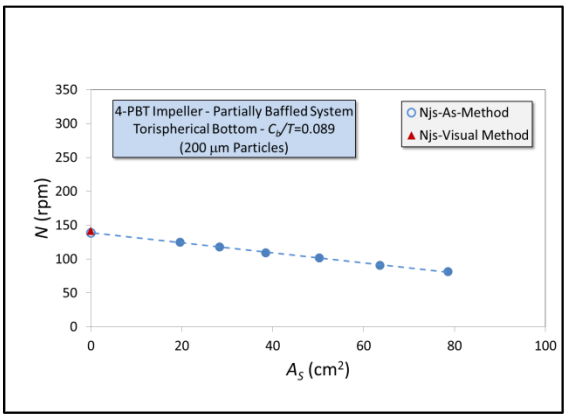

(c)

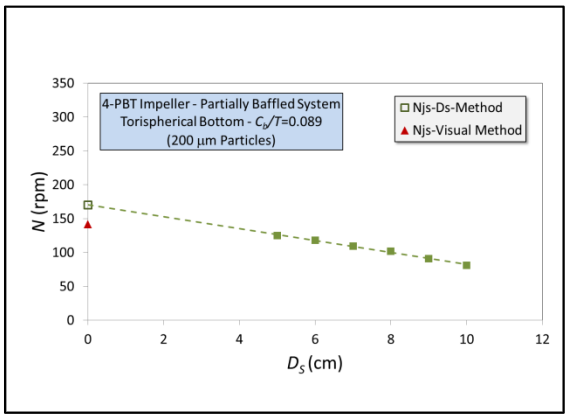

(d)

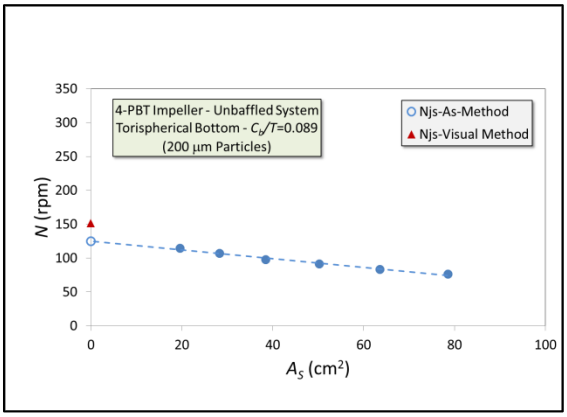

(e)

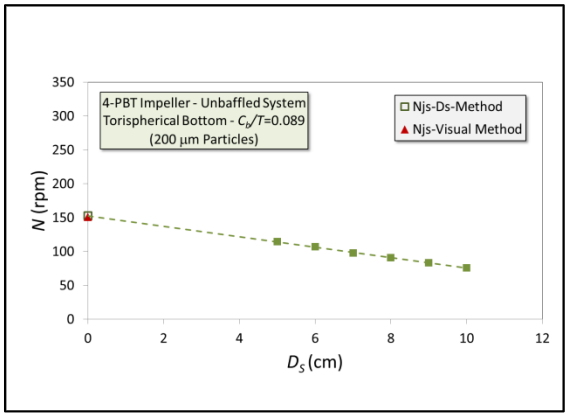

(f)

Figure 3.3 N_{js} measured in the torispherical-bottomed tank with the 4-PBT using for 200 µm particles: (a) $N_{js\text{-}As\text{-}Method}$ in fully baffled system (b) $N_{js\text{-}Ds\text{-}Method}$ in fully baffled system (c) $N_{js\text{-}As\text{-}Method}$ in partially baffled system (d) $N_{js\text{-}Ds\text{-}Method}$ in partially baffled system (e) $N_{js\text{-}As\text{-}Method}$ in unbaffled system (f) $N_{js\text{-}Ds\text{-}Method}$ in unbaffled system.

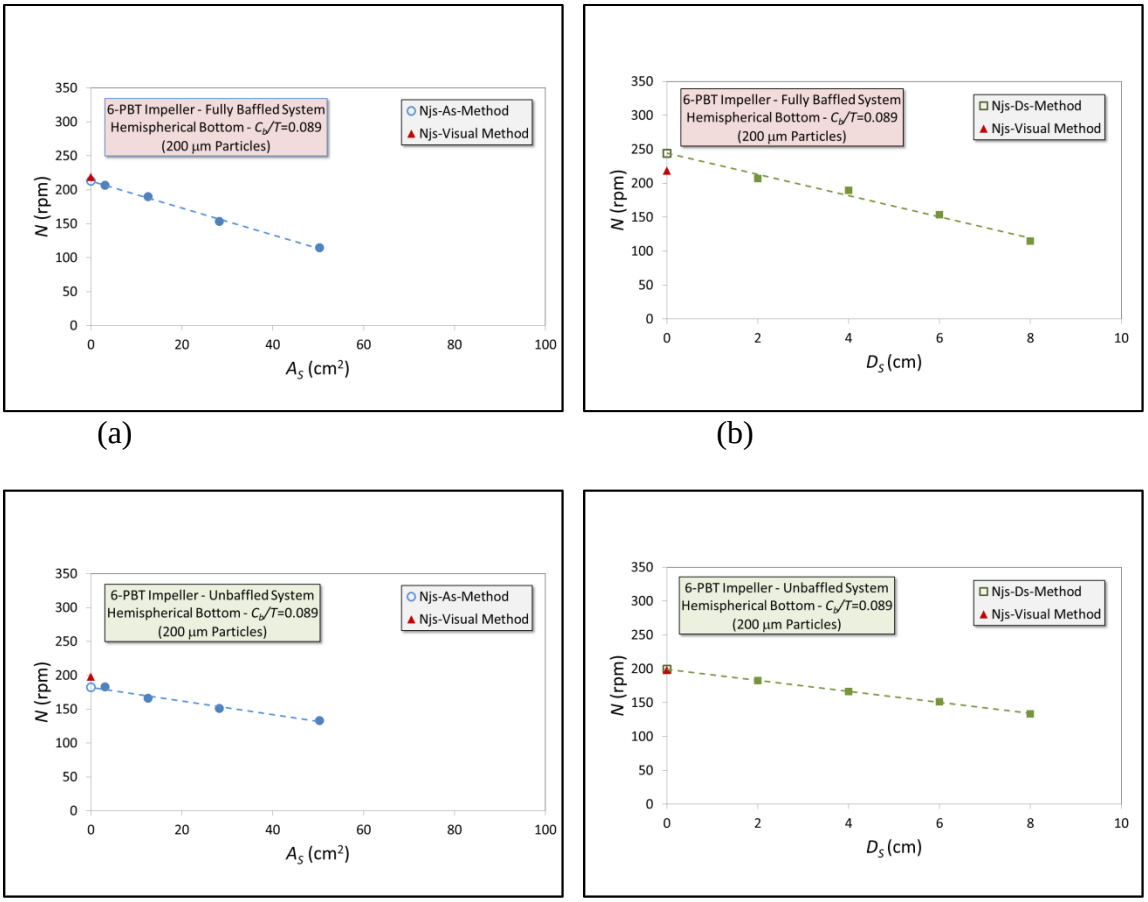

Figure 3.4 N_{js} measured hemispherical-bottomed tank with the 6-PBT using for 200 µm particles: $N_{js\text{-}As\text{-}Method}$ in fully baffled system (b) $N_{js\text{-}Ds\text{-}Method}$ in fully baffled system (c) $N_{js\text{-}As\text{-}Method}$ in unbaffled system (d) $N_{js\text{-}Ds\text{-}Method}$ in unbaffled system.

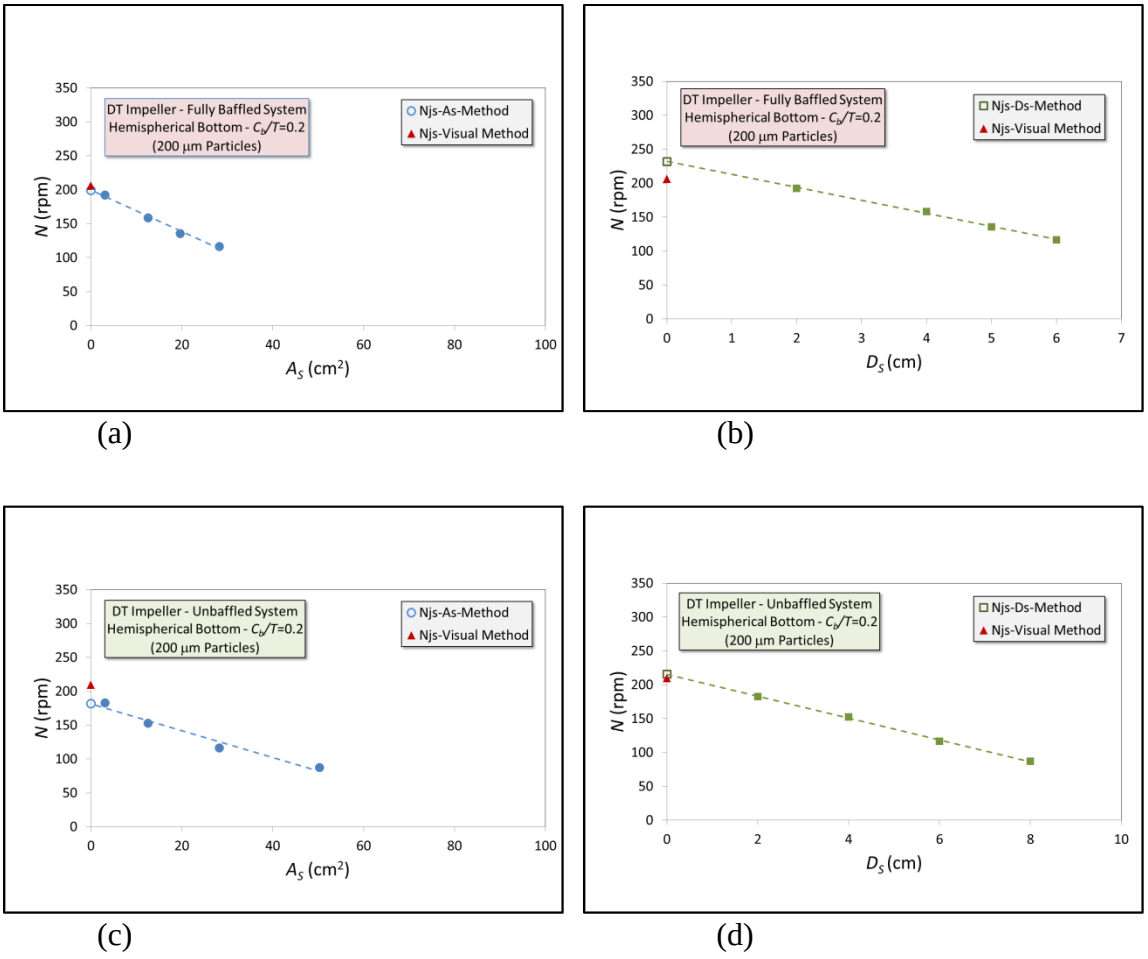

Figure 3.5 N_{js} measured hemispherical-bottomed tank with the 6-PBT using for 200 μm particles: $N_{js\text{-}As\text{-}Method}$ in fully baffled system (b) $N_{js\text{-}Ds\text{-}Method}$ in fully baffled system (c) $N_{js\text{-}As\text{-}Method}$ in unbaffled system (d) $N_{js\text{-}Ds\text{-}Method}$ in unbaffled system.

Additionally, the hemispherical-bottomed tank equipped with either the 6-PBT or the DT under fully baffled and unbaffled configuration was tested. Results of As-method and Ds-method applied to this system are shown in Figure 3.4 and Figure 3.5. The results of these experiments agreed with those of the previous experiments: in fully baffled systems visually determined the N_{js} values were in close agreement with the $N_{js\text{-}As\text{-}Method}$, and in the unbaffled system $N_{js\text{-}Visual}$ was very close to by $N_{js\text{-}Ds\text{-}Method}$.

It can be concluded that the proposed approach to N_{js} determination is valid, at least for the systems tested here, and that this method can be extended to other systems under different operating conditions, as shown below.

3.1.2 N_{js} Results for Different Systems and Operation Conditions

Having preliminarily validated the newly proposed, observed-independent method to N_{js} determination, results for N_{js} were obtained for different systems under different operating conditions.

The results for the RBI system with 150 μm particles for different baffling conditions when the off-bottom ratio (C_b/T) was varied from 0.089 (impeller off-bottom distance = 4cm) to 0.333 (impeller off-bottom distance = 15cm) are presented in Table 3.1. The results show that with fully baffled and partially baffled system N_{js} can be predict by $N_{js\text{-}As\text{-}Method}$, whereas in unbaffled system predictions for N_{js} based on $N_{js\text{-}Ds\text{-}Method}$ are more accurate.

Additionally, results of N_{js} determined with 200 micrometer particles are shown in Table 3.2. Even for these larger particles, the A_S-method works well to determine N_{js} under fully baffled and partially baffled configurations, while the value of N_{js} in unbaffled system is very close to $N_{js\text{-}Ds\text{-}Method}$ obtained value.

Table 3.1 Results for N_{js} with RBI, 150 μm Particles

C_b/T	Particle Size (μm)	Impeller Type	Baffling Type	$N_{js\text{-}Ds\text{-}Method}$ (rpm)	$N_{js\text{-}As\text{-}Method}$ (rpm)	$N_{js\text{-}Visual}$ (rpm)
0.089	150	RBI	Fully Baffled	277.15	242.64	246.44
0.133	150	RBI	Fully Baffled	354.11	314.88	326.66
0.200	150	RBI	Fully Baffled	448.58	399.68	398.74
0.267	150	RBI	Fully Baffled	453.29	397.84	403.54
0.333	150	RBI	Fully Baffled	440.55	395.39	403.24
0.089	150	RBI	Partially Baffled	190.92	161.04	166.96
0.089	150	RBI	Unbaffled	182.74	145.11	178.24
0.133	150	RBI	Unbaffled	203.58	154.99	197.04
0.200	150	RBI	Unbaffled	230.73	171.12	221.92
0.267	150	RBI	Unbaffled	177.2	141.07	186.58
0.333	150	RBI	Unbaffled	196.49	152.46	204.02

Table 3.2 Results for N_{js} with RBI, 200 μm Particles

C_b/T	Particle Size (μm)	Impeller Type	Baffling Type	$N_{js\text{-}Ds\text{-}Method}$ (rpm)	$N_{js\text{-}As\text{-}Method}$ (rpm)	$N_{js\text{-}Visual}$ (rpm)
0.089	200	RBI	Fully Baffled	325.78	293.14	296.12
0.133	200	RBI	Fully Baffled	414.6	376.36	383.76
0.200	200	RBI	Fully Baffled	487.22	446.99	444.74
0.267	200	RBI	Fully Baffled	448.19	415.16	419.12
0.333	200	RBI	Fully Baffled	468.17	429.79	446.9
0.089	200	RBI	Partially Baffled	253.04	208.96	204.04
0.089	200	RBI	Unbaffled	209.74	167.95	208.3
0.133	200	RBI	Unbaffled	220.04	174.74	218.26
0.200	200	RBI	Unbaffled	233.45	181.23	228.62
0.267	200	RBI	Unbaffled	227.64	181.64	222.64
0.333	200	RBI	Unbaffled	236.89	187.01	228.58

Table 3.3 Results for N_{js} with 4-PBT, 200 μm Particles

C_b/T	Particle Size (μm)	Impeller Type	Baffling Type	$N_{js\text{-}Ds\text{-}Method}$ (rpm)	$N_{js\text{-}As\text{-}Method}$ (rpm)	$N_{js\text{-}Visual}$ (rpm)
0.089	200	4-PBT	Fully Baffled	154.36	132	136.72
0.133	200	4-PBT	Fully Baffled	159.74	139.31	142.62
0.200	200	4-PBT	Fully Baffled	168.19	147.89	149.36
0.267	200	4-PBT	Fully Baffled	178.16	155.05	159.7
0.333	200	4-PBT	Fully Baffled	185.8	164.77	169.52
0.089	200	4-PBT	Partially Baffled	170.31	138.96	141.74
0.089	200	4-PBT	Unbaffled	152.79	125.05	151.32
0.133	200	4-PBT	Unbaffled	162.32	131.33	157.42
0.200	200	4-PBT	Unbaffled	161.59	131.11	159.98
0.267	200	4-PBT	Unbaffled	172.56	139.56	169.36
0.333	200	4-PBT	Unbaffled	199.75	160.72	191.84

Table 3.4 Results for N_{js} with 6-PBT, 200 μm Particles

C_b/T	Particle Size (μm)	Impeller Type	Baffling Type	$N_{js\text{-}Ds\text{-}Method}$ (rpm)	$N_{js\text{-}As\text{-}Method}$ (rpm)	$N_{js\text{-}Visual}$ (rpm)
0.089	200	6-PBT	Fully Baffled	244.24	212.83	218.64
0.133	200	6-PBT	Fully Baffled	269.83	240.54	250.72
0.200	200	6-PBT	Fully Baffled	275.44	246.46	255
0.267	200	6-PBT	Fully Baffled	279.94	254.51	253.76
0.333	200	6-PBT	Fully Baffled	300.86	275.64	285.08
0.089	200	6-PBT	Unbaffled	199.14	182.21	198.12
0.133	200	6-PBT	Unbaffled	213.13	193.53	210.58
0.200	200	6-PBT	Unbaffled	206.36	186.12	207.68
0.267	200	6-PBT	Unbaffled	200.12	181.36	200.98
0.333	200	6-PBT	Unbaffled	192.12	175.36	193.54

Table 3.5 Results for N_{js} with DT, 200 μm Particles

C_b/T	Particle Size (μm)	Impeller Type	Baffling Type	$N_{js\text{-}Ds\text{-}Method}$ (rpm)	$N_{js\text{-}As\text{-}Method}$ (rpm)	$N_{js\text{-}Visual}$ (rpm)
0.200	200	DT	Fully Baffled	232.03	199.25	206.12
0.267	200	DT	Fully Baffled	204.28	182.54	190.4
0.333	200	DT	Fully Baffled	219.04	192.55	200.58
0.200	200	DT	Unbaffled	215.31	181.56	209.56
0.267	200	DT	Unbaffled	226.02	188.8	220.1
0.333	200	DT	Unbaffled	224.32	186.68	224.18

In order to better visualize these results, parity plots were generated using the visual values for N_{js} vs. those obtained with the proposed method. The results are presented in Figure 3.6. Panels (a)-(d) show the data for specific systems, whereas Figure 3.6(e) shows the results for all data systems. The closer the points align themselves on a 45º-angle-line the better the agreement. In all cases, one can see that the values of $N_{js\text{-}Visual}$ agree well with those for $N_{js\text{-}As\text{-}method}$ for the fully baffled and partially baffled systems and $N_{js\text{-}Ds\text{-}method}$ for the unbaffled systems. The R-value for all the points is 0.999.

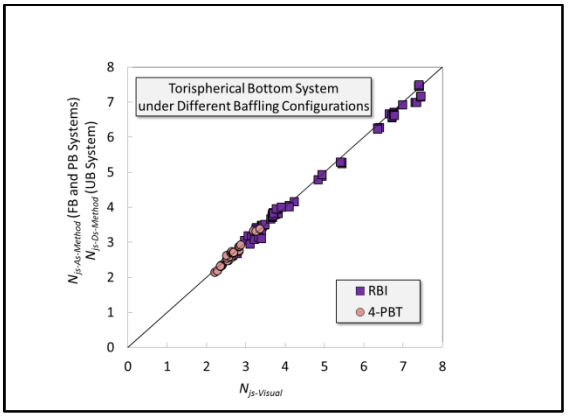
Torispherical Bottom System
under Different Baffling Configurations
RBI
4-PBT
$N_{js\text{-}As\text{-}Method}$ (FB and PB Systems)
$N_{js\text{-}Ds\text{-}Method}$ (UB System)
$N_{js\text{-}Visual}$

(a)

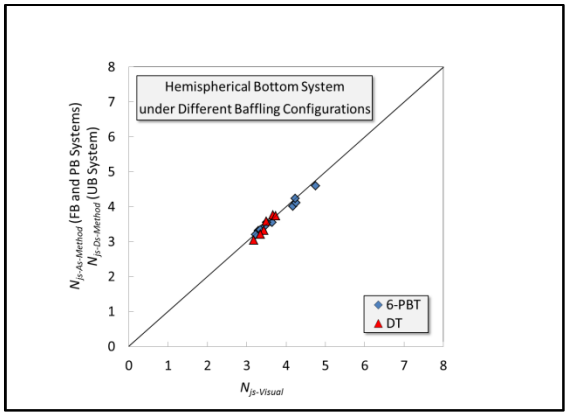
Hemispherical Bottom System
under Different Baffling Configurations
6-PBT
DT
$N_{js\text{-}As\text{-}Method}$ (FB and PB Systems)
$N_{js\text{-}Ds\text{-}Method}$ (UB System)
$N_{js\text{-}Visual}$

(b)

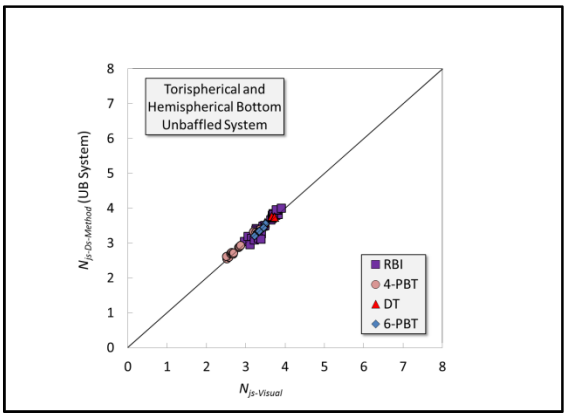
Torispherical and
Hemispherical Bottom
Unbaffled System
RBI
4-PBT
DT
6-PBT
$N_{js\text{-}Ds\text{-}Method}$ (UB System)
$N_{js\text{-}Visual}$

(c)

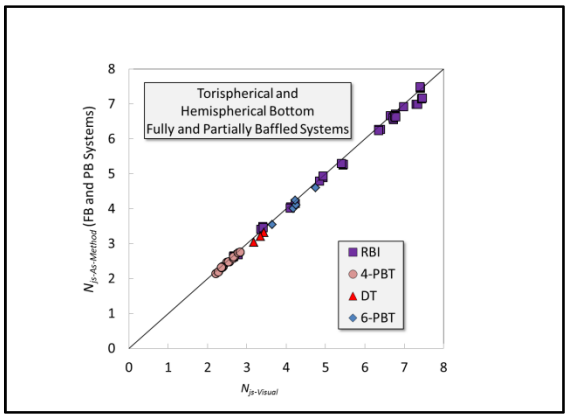
Torispherical and
Hemispherical Bottom
Fully and Partially Baffled Systems
RBI
4-PBT
DT
6-PBT
$N_{js\text{-}As\text{-}Method}$ (FB and PB Systems)
$N_{js\text{-}Visual}$

(d)

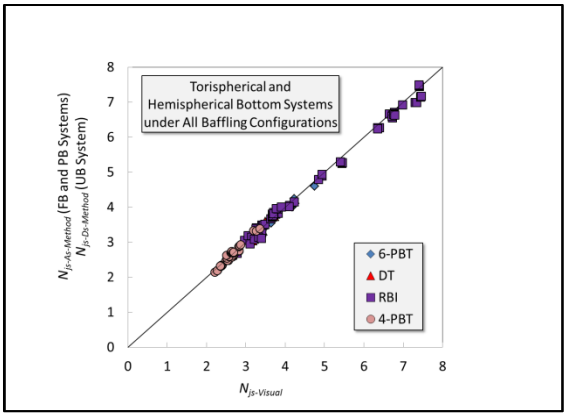

(e)

Figure 3.6 Parity plots of $N_{js\text{-}As\text{-}Method}$ (for fully baffled (FB) and partially baffled (PB) systems) and $N_{js\text{-}Ds\text{-}Method}$ (for unbaffled (UB) systems) vs. $N_{js\text{-}Visual}$. (a) Parity plot for all torispherical-bottom systems (b) Parity plot for all hemispherical-bottom systems (c) Parity plot for all unbaffled systems (d) Parity plot for all fully baffled and partially baffled systems (e) parity plot for all data.

3.1.3 Comparison of the Effect of the Impeller Off-bottom Clearance Ration C_b/T on the Minimum Agitation Speed for Solid Suspension N_{js} for Different Mixing Systems

The values of N_{js} were experimentally obtained for different C_b/T ratios for all four systems (torispherical-bottomed tank with retreat blade impeller system, torispherical-bottomed tank with four-blade pitched-blade turbine, hemispherical-bottomed tank with six-blade pitched-blade turbine and hemispherical-bottomed tank with 6-disk turbine). The results with the 150 µm particles and 200 µm particles as dispersed phase are shown in Figure 3.7(a) and 3.7(b), respectively. This figure shows that in the fully baffled system, N_{js} increase sharply with C_b/T for C_b/T<0.2 and remains nearly constant for C_b/T>0.2. Also, it is evident that N_{js} in the fully baffled system is much higher than in the other two baffling types. Panels (c) (d) and (e) in Figure 3.7 show that the effects of both baffling type and C_b/T on then minimum agitation speed are relatively small, especially using 4-PBT impeller. Triplicates experiment were conducted with RBI and 4-PBT impellers and the standard deviation of triplicate data was calculated for each point. The typical standard

deviation was too small (<1%) to be plotted, indicating that the results were highly reproducible.

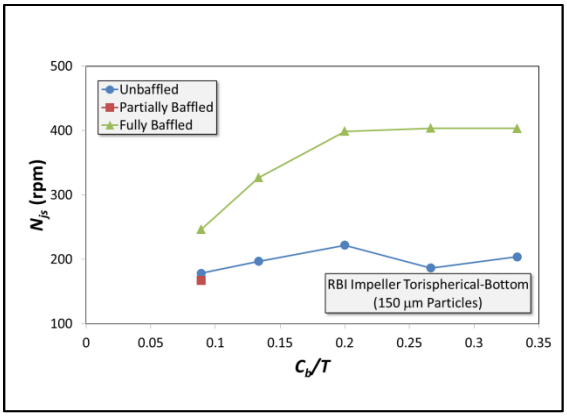

(a)

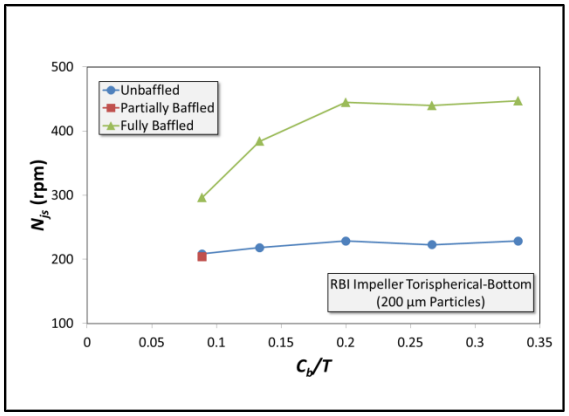

(b)

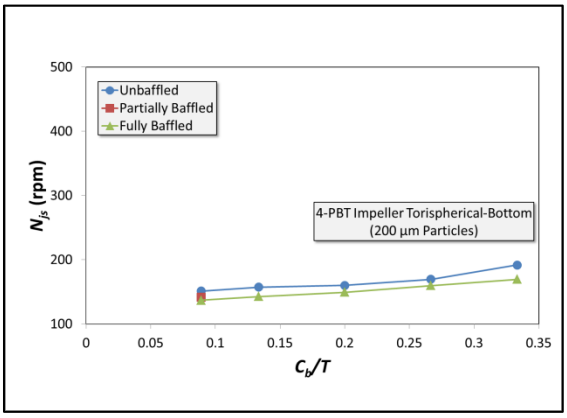

(c)

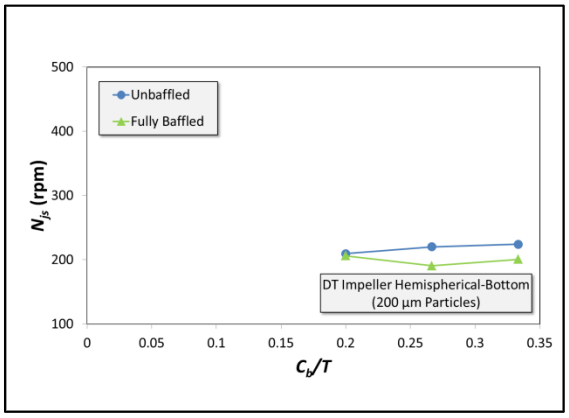

(d)

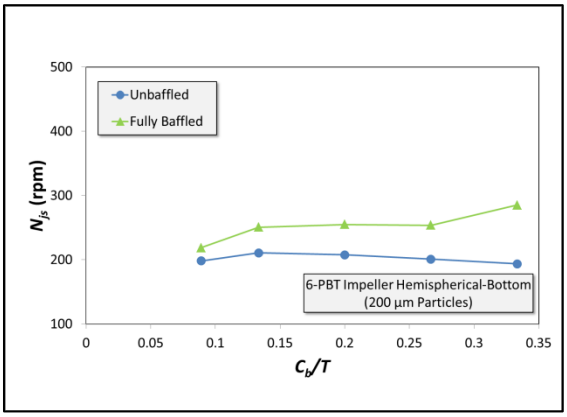

(e)

Figure 3.7 Effect of the impeller off-bottom clearance ratio C_b/T on N_{js} for different baffling configurations: (a) RBI (150 µm particles) (b) RBI (200 µm particles) (c) 4-PBT (200 µm particles) (d) DT (200 µm particles) (e) 6-PBT (200 µm particles).

3.1.4 Power Dissipation at N_{js}

The results for the impeller power dissipation at N_{js} are shown in the Appendix. For all four impellers, the highest power consumption to achieve the solids just suspended state occurred when the tank was fully baffled. A comparison of the power consumed at N_{js} by each impeller in the same tank system shows that using the 4-PBT in the torispherical tank was more efficient than using the RBI. For the hemispherical-bottom tank, the system equipped with 6-PBT used in this work was more efficient than that with the DT.

In mixing systems, it is customary to use the Power Number, Po, defined as:

$$Po = \frac{P}{\rho N^3 D^5}$$

to express the power dissipated by the impeller in a non-dimensional form. Plots of Po at N_{js} (defined as Po_{js} here) vs. C_b/T are shown in Figure 3.8.

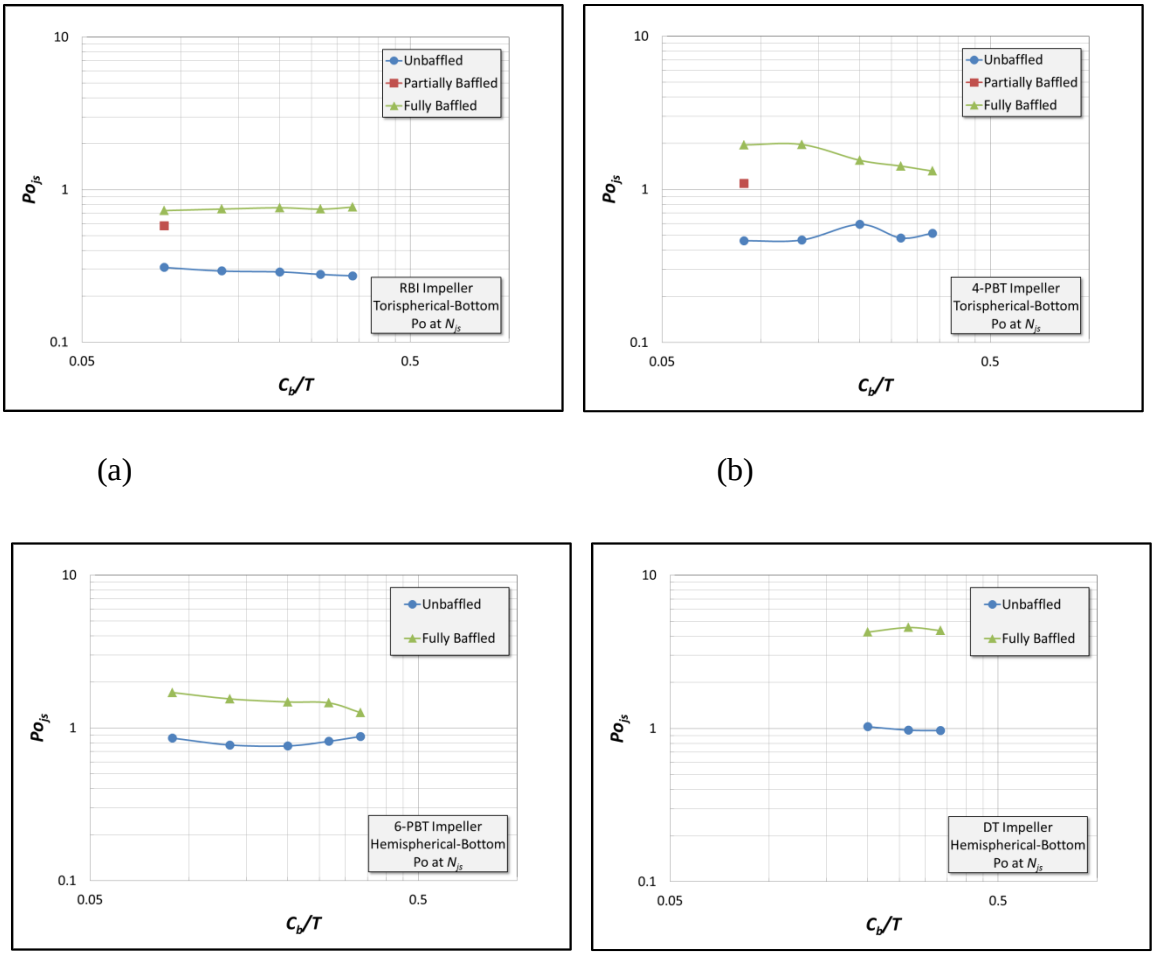

Figure 3.8 Impeller power number Po_{js} at different C_b/T values: (a) RBI impeller (b) 4-PBT Impeller (c) 6-PBT impeller (d) DT impeller.

3.1.5 S-Value for Zwietering Equation

Based on the Zwietering Equation:

$$N_{js} = s\frac{\nu^{0.1} d_p^{0.2} \left(g\Delta\rho/\rho_L\right)^{0.45} X^{0.13}}{D^{0.85}}$$

The S-values were obtained by fitting the experimental Njs data to this equation using as densities 2572 kg/m^3 and 997.537 kg./m^3 for the glass particles (measured separately via a pycnometer) and for water, respectively. Figure 3.9 shows S-value vs. C_b/T for different systems.

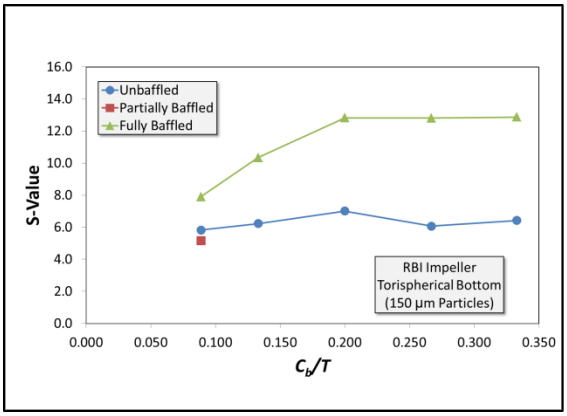

(a)

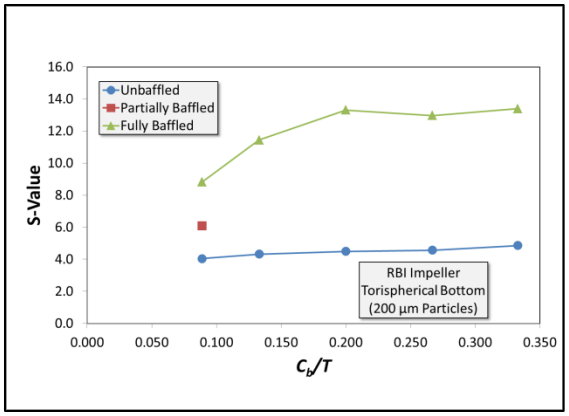

(b)

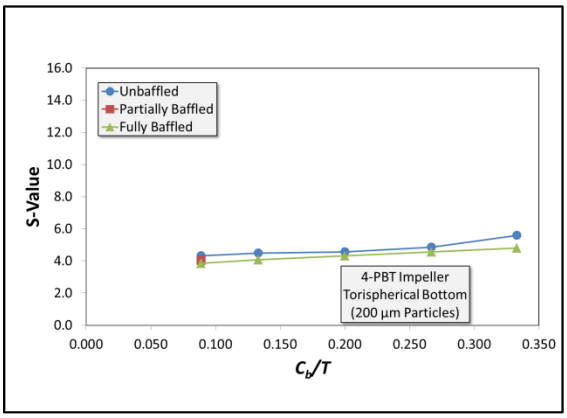

(c)

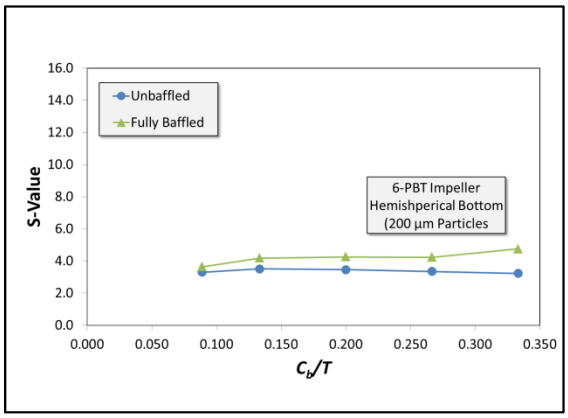

(d)

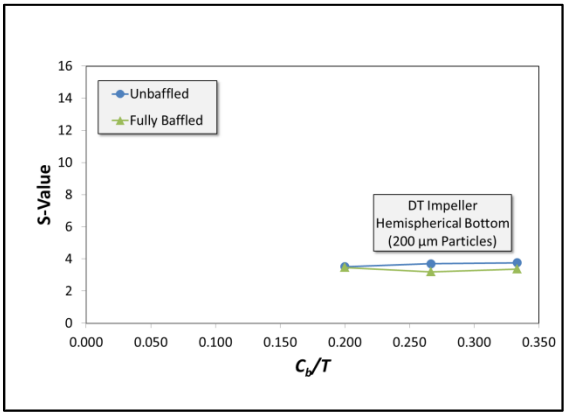

(e)

Figure 3.9 S-values for Zwithering equation. (a) RBI (150 µm particles) (b) 200 RBI (µm particles) (c) 4-PBT (200 µm particles) (d) 6-PBT (200 µm particles) (e) DT (200 µm particles).

3.2 Power Dissipation for Mixing System

Power dissipation data and power numbers for RBI, 4-PBT, 6-PBT and DT are experimentally determined by different baffling conditions and impeller off-bottom ration C_b/T. Results are shown in Figure3.9, Figure3.10, Figure 3.11, Figure 3.12 and Figure 3.13. Power number obtained by this work were in good agreement with the limited literature data available.

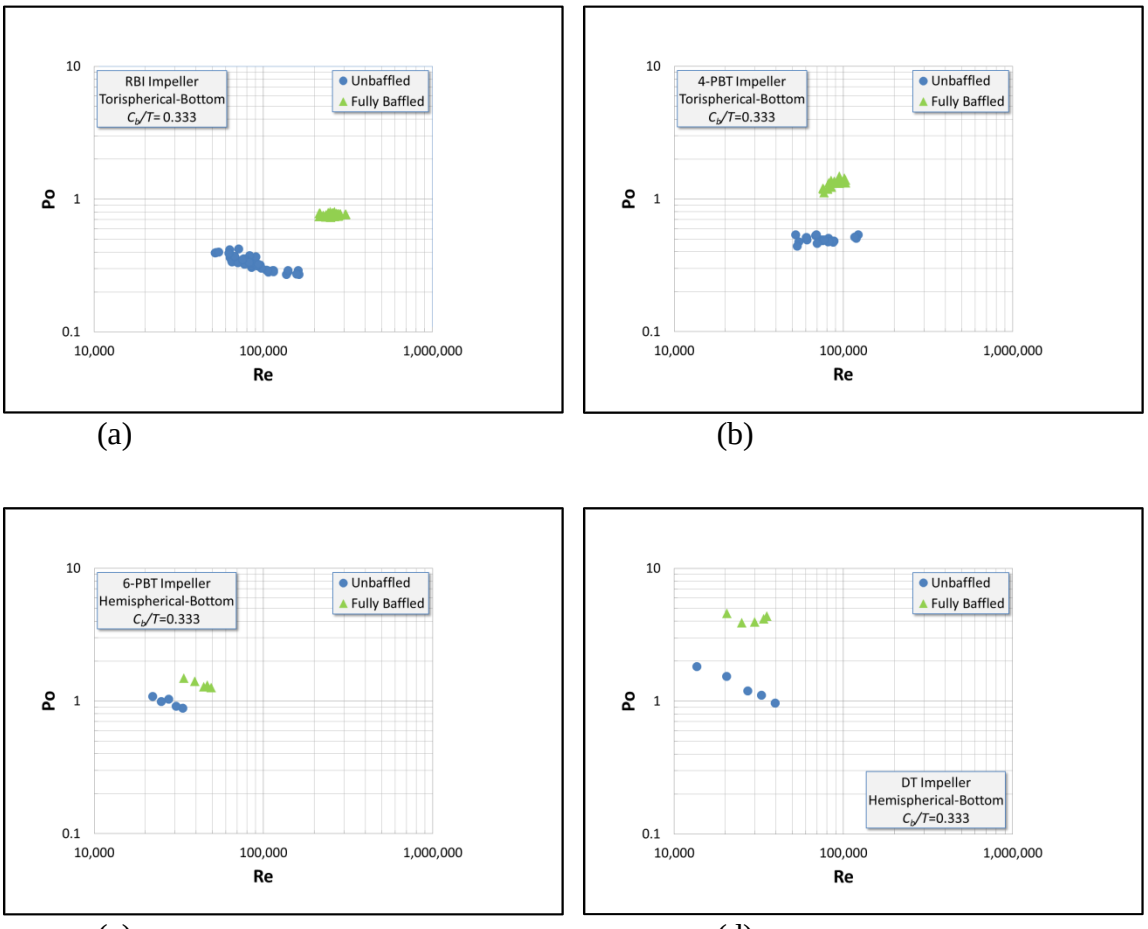

Figure 3.10 Power number at C_b/T = 0.333 (a) RBI impeller (b) 4-PBT impeller (c)6-PBT impeller (d) DT impeller.

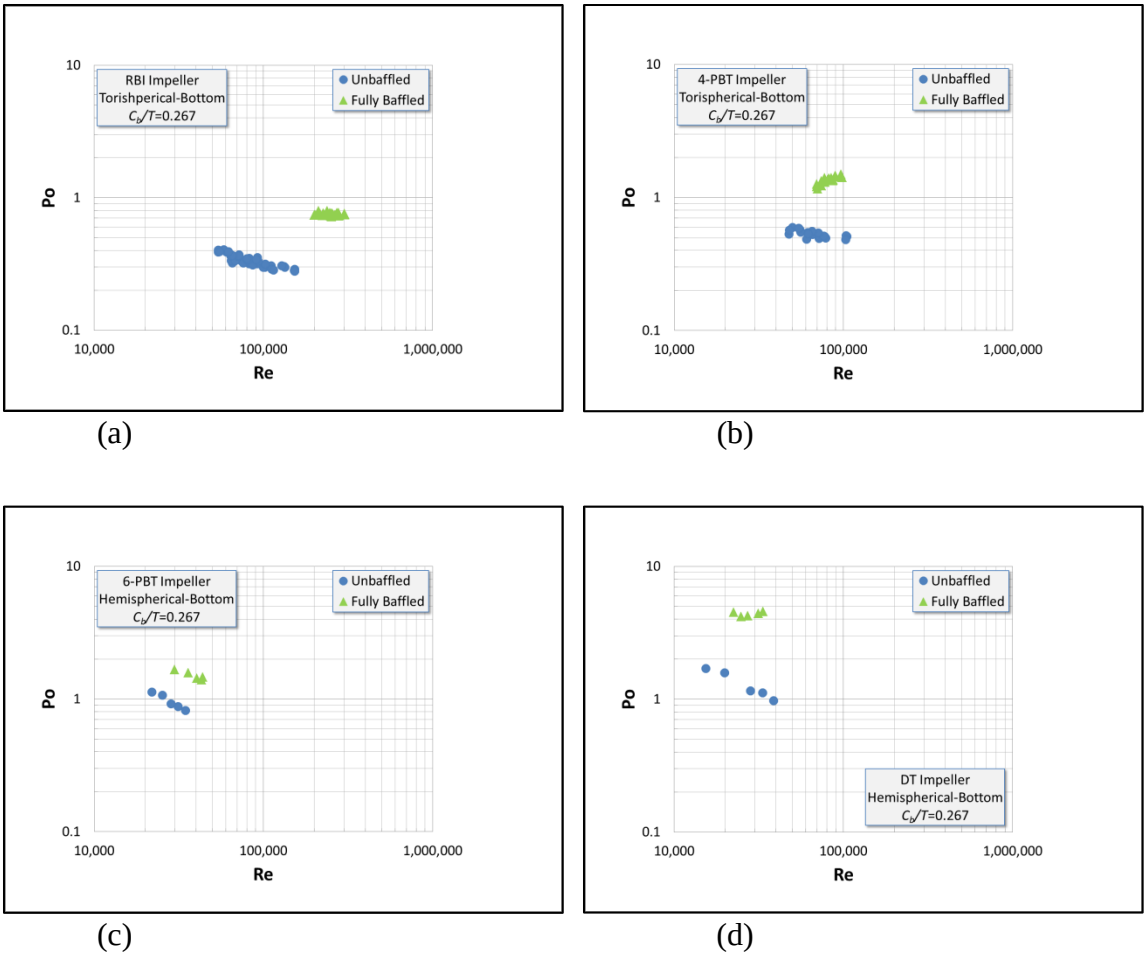

Figure 3.11 Power number at C_b/T = 0.267 (a) RBI impeller (b) 4-PBT impeller (c) 6-PBT impeller (d) DT impeller.

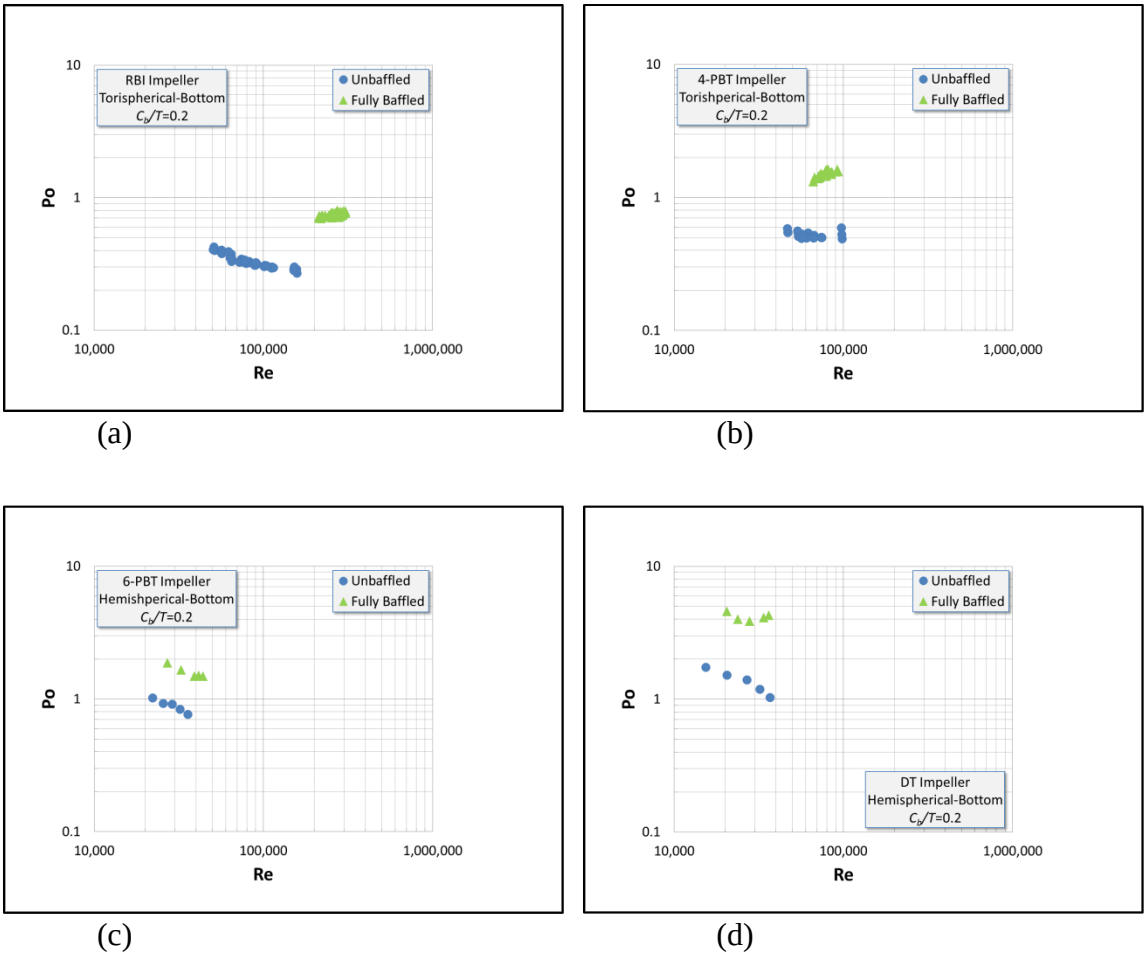

Figure 3.12 Power number at C_b/T = 0.2 (a) RBI impeller (b) 4-PBT impeller (c) 6-PBT impeller (d) DT impeller.

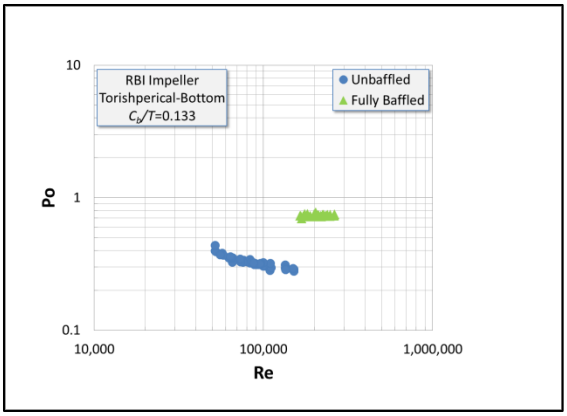

(a)

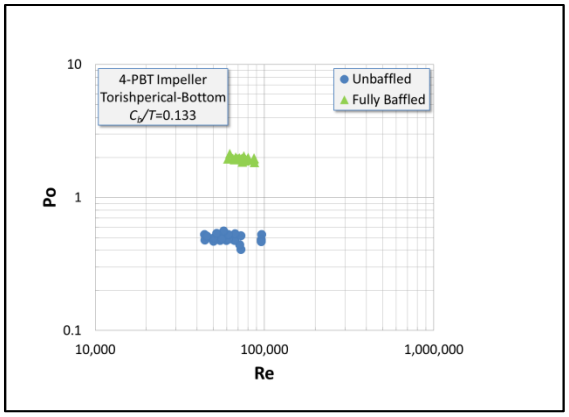

(b)

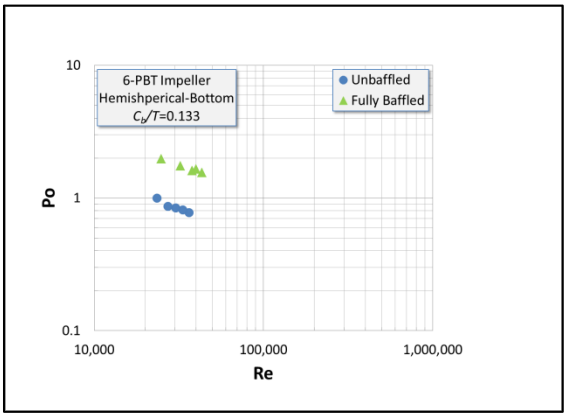

(c)

Figure 3.13 Power number at C_b/T = 0.133 (a) RBI impeller (b) 4-PBT impeller (c) 6-PBT impeller.

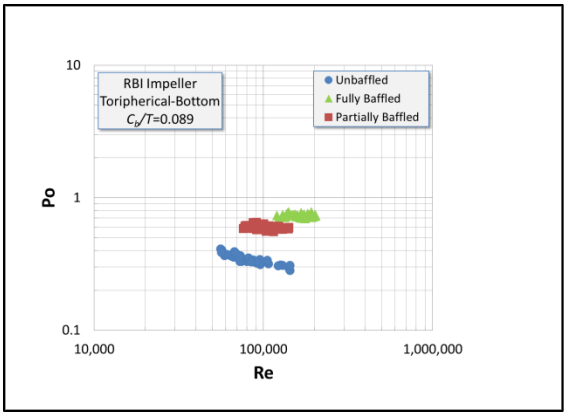

(a)

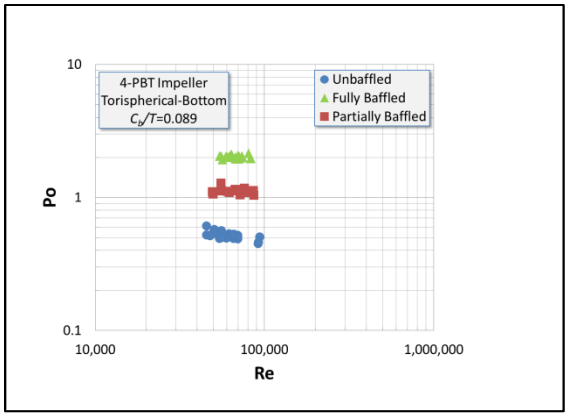

(b)

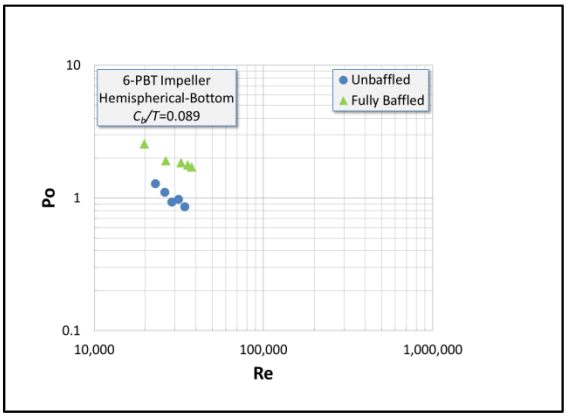

(c)

Figure 3.14 Power number at C_b/T = 0.089 (a) RBI impeller (b) 4-PBT impeller (c) 6-PBT impeller.

CHAPTER 4

CONCLUSION

In this work, the minimum agitation speed to achieve solid suspension in vessels commonly used in the pharmaceutical industry as reactors was experimentally obtained using four different types of impellers, i.e., retreat curve-blade impeller, four-blade pitched-blade turbine, six-blade pitched-blade turbine and six-blade disk turbine under fully baffled, partially baffled and unbaffled configurations. A novel method for determination of minimum agitation speed, N_{js}, was obtained (Njs-As-Method and Njs-Ds-Method). The Njs-As-Method can be used for fully baffled and partially baffled system; Njs-Ds-Method can be used for unbaffled system. The new method works well in the precise determination of N_{js} in torispherical- and hemispherical-bottomed tank systems. Triplicates experiment were conducted with RBI and 4-PBT, and the small standard deviation for N_{js} is an indication the novel approach is highly replicable.

It was found that the value of N_{js} for the RBI under fully baffled conditions increased significantly with increasing values of C_b/T. However, for the other baffling configurations and impellers, N_{js} change only slightly with impeller C_b/T.

The power dissipated at the minimum agitation speed for off-bottom solid suspension were also obtained for different C_b/T values, impellers types, and baffling configurations. The results show that the highest power dissipations were obtained with the RBI under fully baffled system. For the other situations, power dissipation is much lower. The results obtained in this work are directly applicable to the pharmaceutical industry where these reactors are commonly used.

APPENDIX

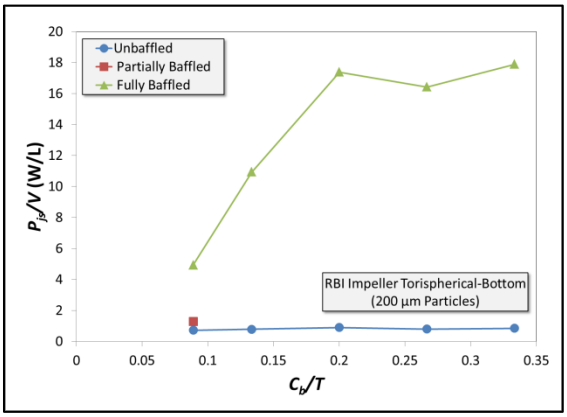

(a)

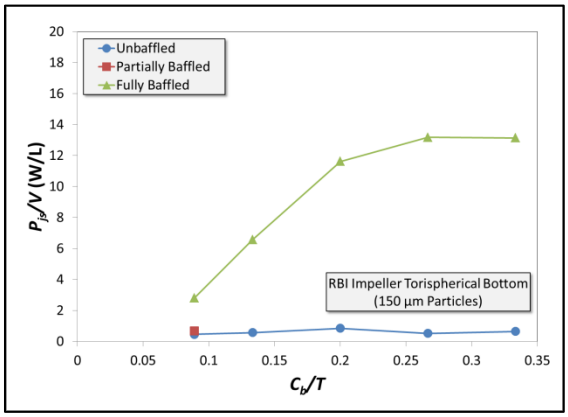

(b)

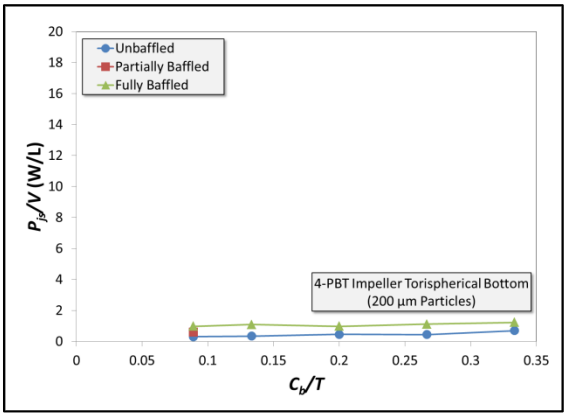

(c)

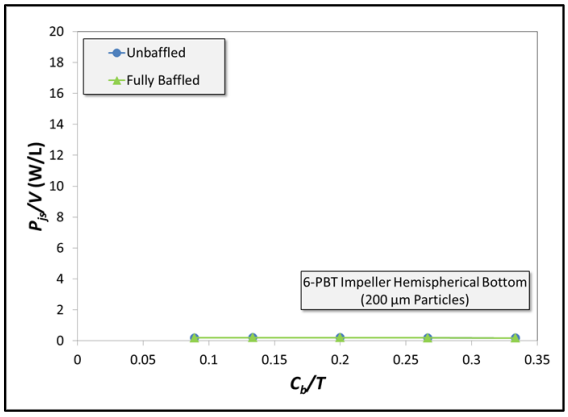

(d)

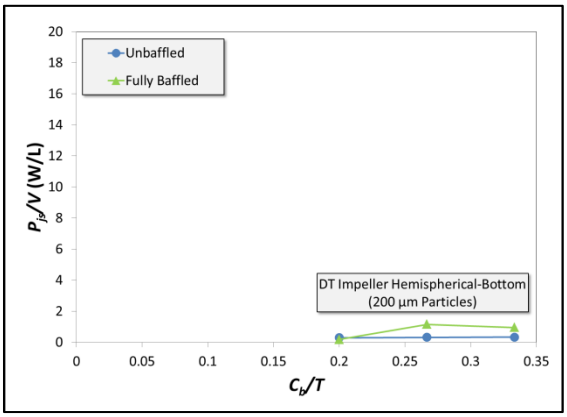

(e)

Figure A1 Impeller consumption at N_{js} for all systems

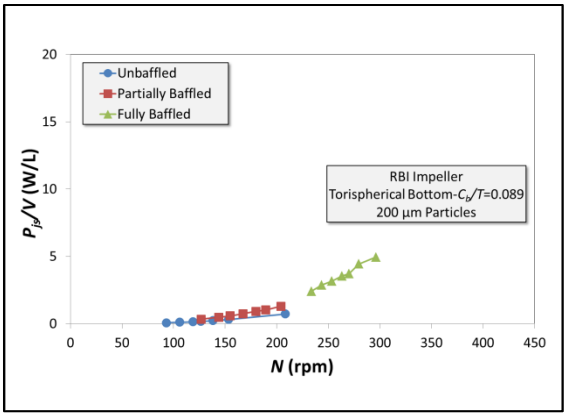
Unbaffled
Partially Baffled
Fully Baffled
RBI Impeller
Torispherical Bottom-C_b/T=0.089
200 µm Particles
P_{js}/V (W/L)
N (rpm)

(a)

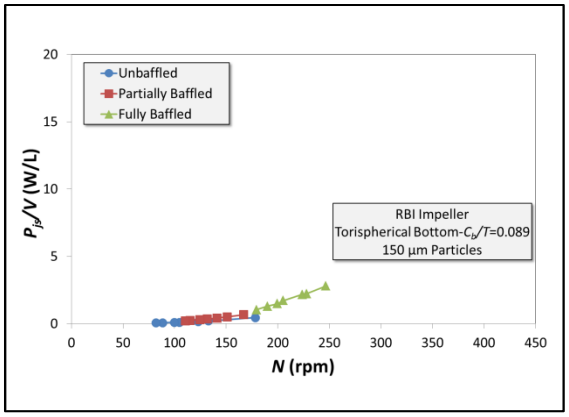
Unbaffled
Partially Baffled
Fully Baffled
RBI Impeller
Torispherical Bottom-C_b/T=0.089
150 µm Particles
P_{js}/V (W/L)
N (rpm)

(b)

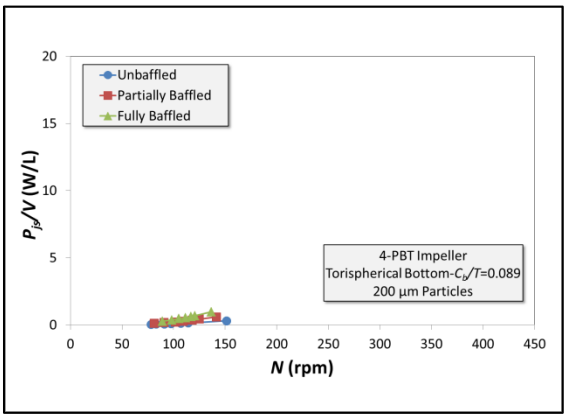
Unbaffled
Partially Baffled
Fully Baffled
4-PBT Impeller
Torispherical Bottom-C_b/T=0.089
200 µm Particles
P_{js}/V (W/L)
N (rpm)

(c)

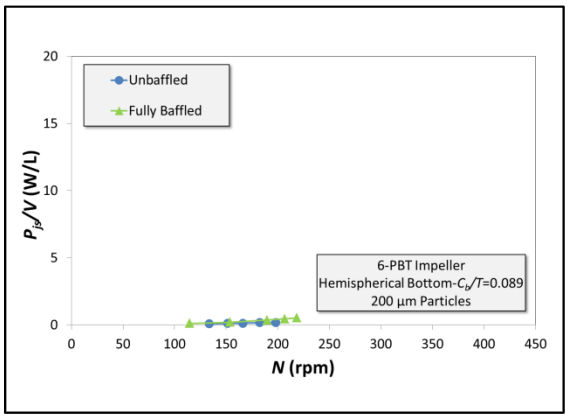
Unbaffled
Fully Baffled
6-PBT Impeller
Hemispherical Bottom-C_b/T=0.089
200 µm Particles
P_{js}/V (W/L)
N (rpm)

(d)

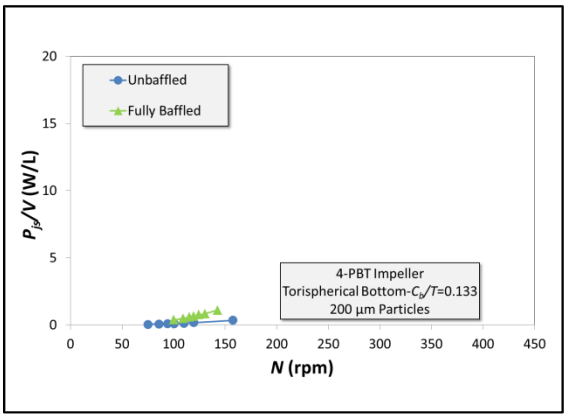
Unbaffled
Fully Baffled
4-PBT Impeller
Torispherical Bottom-C_b/T=0.133
200 µm Particles
P_{js}/V (W/L)
N (rpm)

(e)

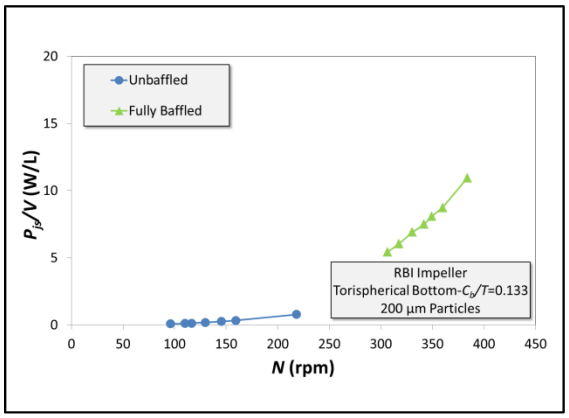
Unbaffled
Fully Baffled
RBI Impeller
Torispherical Bottom-C_b/T=0.133
200 µm Particles
P_{js}/V (W/L)
N (rpm)

(f)

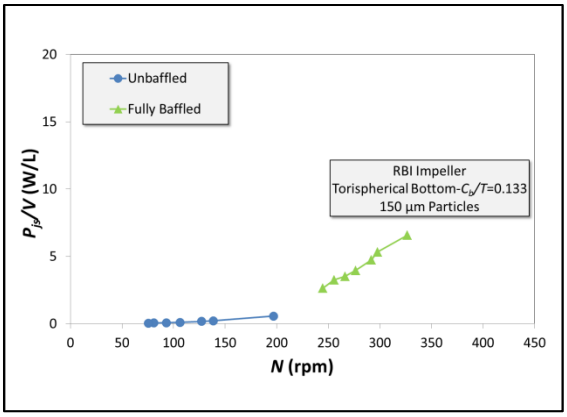
Unbaffled
Fully Baffled
RBI Impeller
Torispherical Bottom-C_b/T=0.133
150 µm Particles
P_{js}/V (W/L)
N (rpm)

(g)

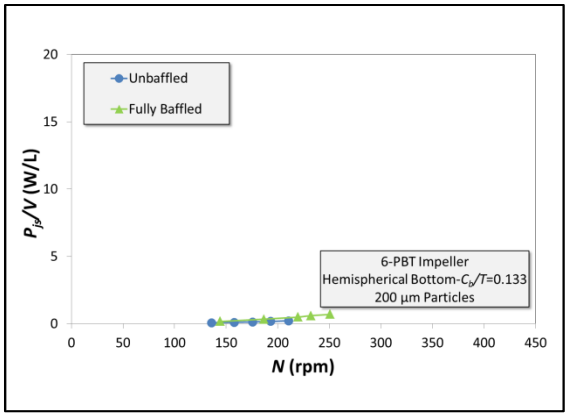
Unbaffled
Fully Baffled
6-PBT Impeller
Hemispherical Bottom-C_b/T=0.133
200 µm Particles
P_{js}/V (W/L)
N (rpm)

(h)

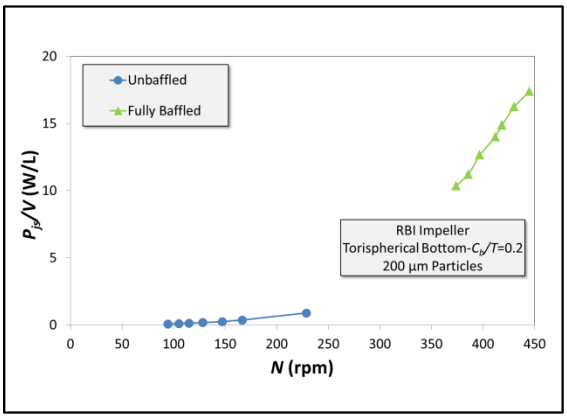
Unbaffled
Fully Baffled
RBI Impeller
Torispherical Bottom-C_b/T=0.2
200 µm Particles
P_{js}/V (W/L)
N (rpm)

(i)

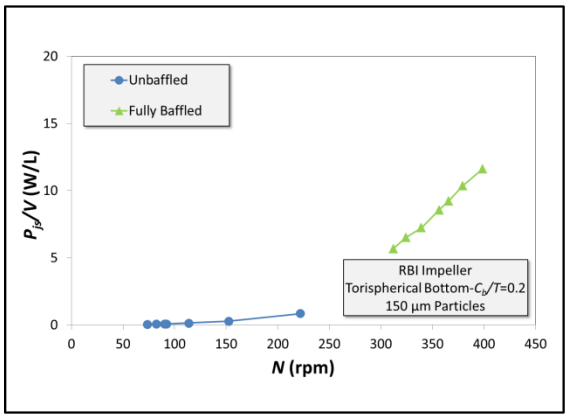
Unbaffled
Fully Baffled
RBI Impeller
Torispherical Bottom-C_b/T=0.2
150 µm Particles
P_{js}/V (W/L)
N (rpm)

(j)

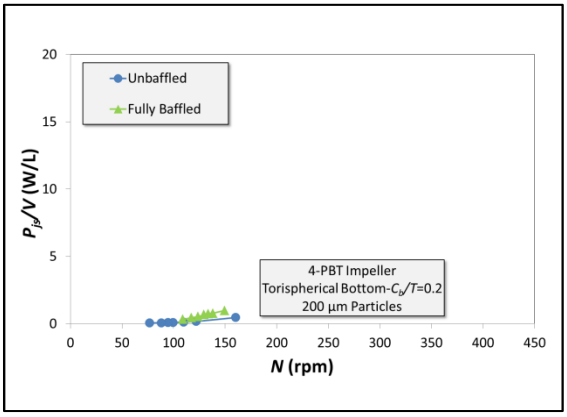
Unbaffled
Fully Baffled
4-PBT Impeller
Torispherical Bottom-C_b/T=0.2
200 µm Particles
P_{js}/V (W/L)
N (rpm)

(k)

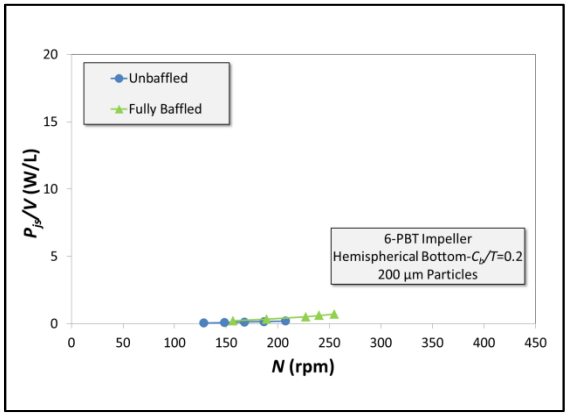
Unbaffled
Fully Baffled
6-PBT Impeller
Hemispherical Bottom-C_b/T=0.2
200 µm Particles
P_{js}/V (W/L)
N (rpm)

(l)

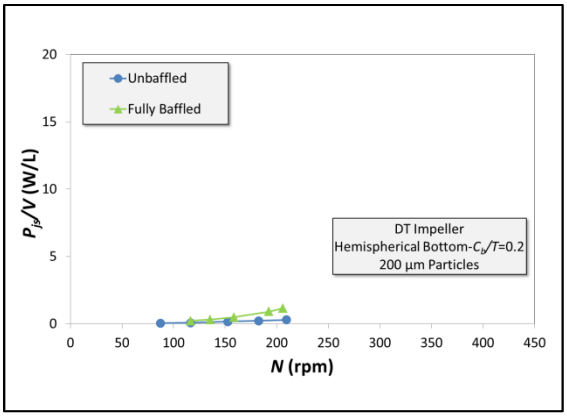
Unbaffled
Fully Baffled
DT Impeller
Hemispherical Bottom-C_b/T=0.2
200 µm Particles
P_{js}/V (W/L)
N (rpm)

(m)

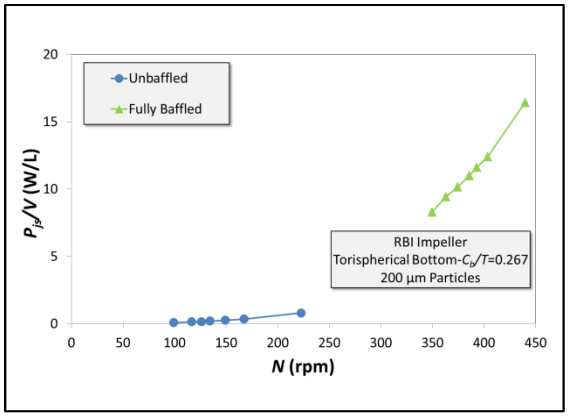
Unbaffled
Fully Baffled
RBI Impeller
Torispherical Bottom-C_b/T=0.267
200 µm Particles
P_{js}/V (W/L)
N (rpm)

(n)

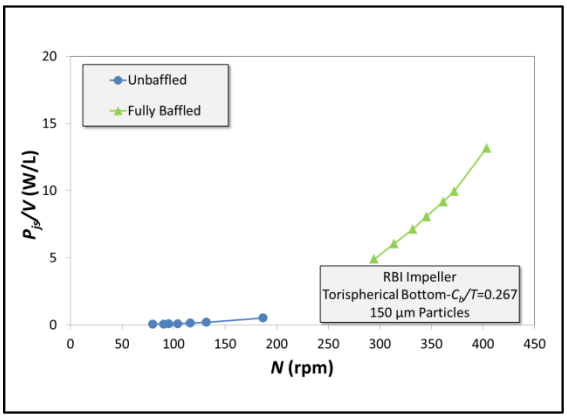
Unbaffled
Fully Baffled
RBI Impeller
Torispherical Bottom-C_b/T=0.267
150 µm Particles
P_{js}/V (W/L)
N (rpm)

(o)

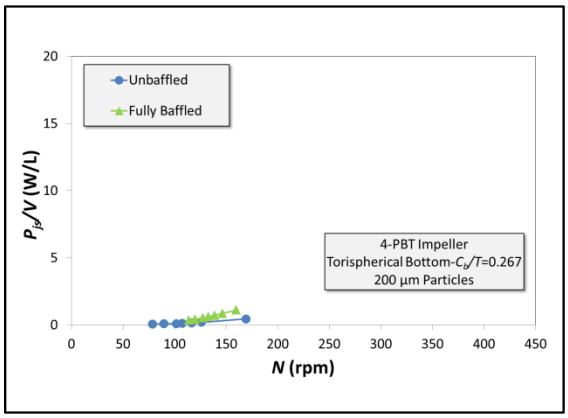
Unbaffled
Fully Baffled
4-PBT Impeller
Torispherical Bottom-C_b/T=0.267
200 µm Particles
P_{js}/V (W/L)
N (rpm)

(p)

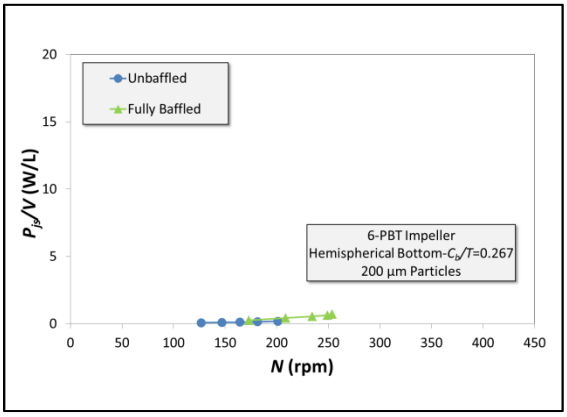
Unbaffled
Fully Baffled
6-PBT Impeller
Hemispherical Bottom-C_b/T=0.267
200 µm Particles
P_{js}/V (W/L)
N (rpm)

(q)

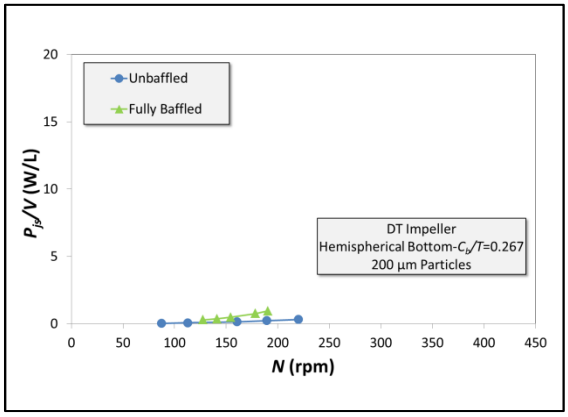
Unbaffled
Fully Baffled
DT Impeller
Hemispherical Bottom-C_b/T=0.267
200 µm Particles
P_{js}/V (W/L)
N (rpm)

(r)

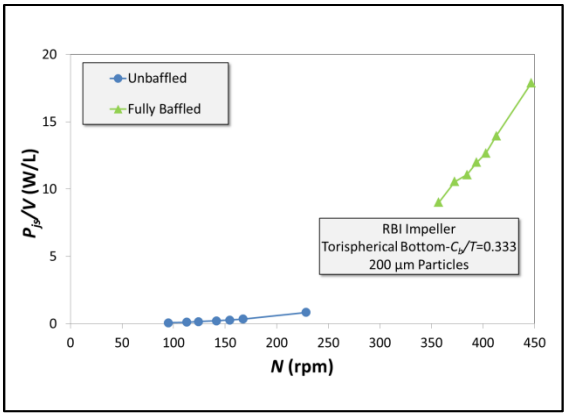

(s)

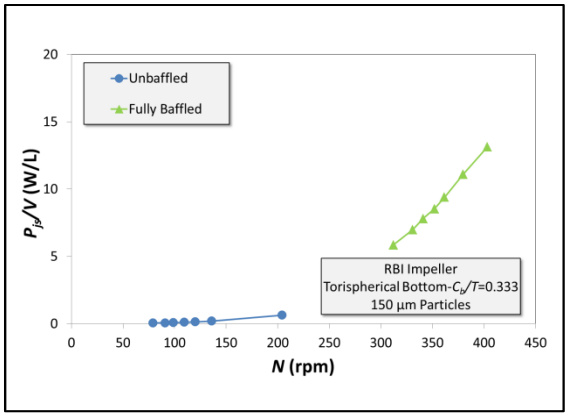

(t)

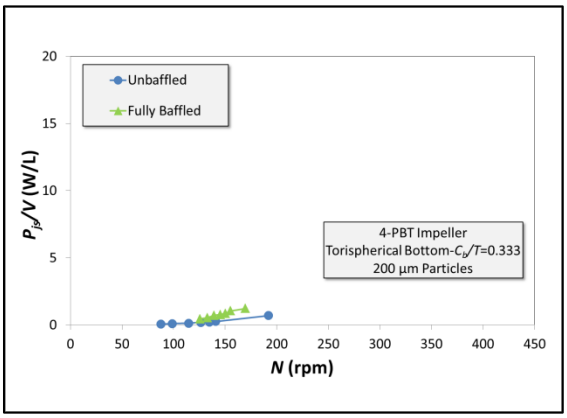

(u)

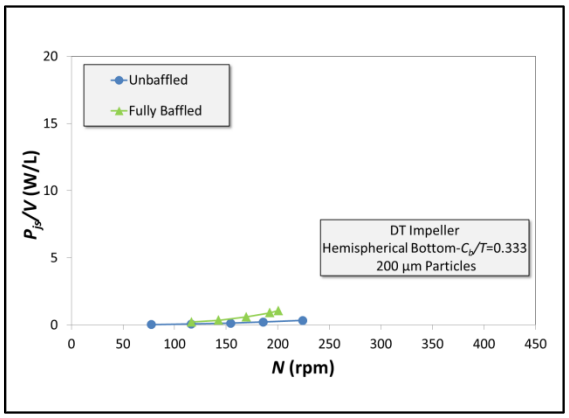

(v)

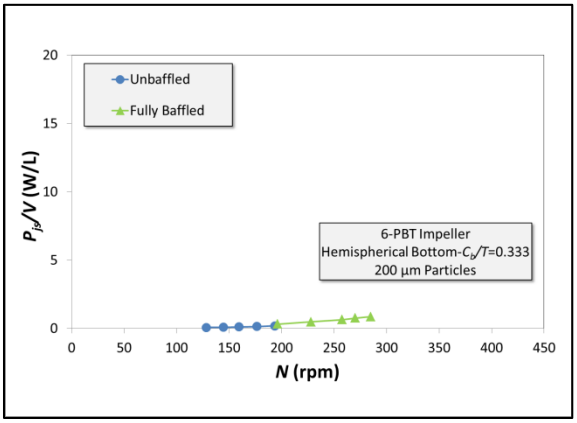

(w)

Figure A2 Power consumption by each system

Table A1 S-Value from Zwietering Equation

Impeller Type	Type of Tank Bottom	Baffling Type	Particle Size, dp (m)	Impeller Diameter, D (m)	S-Value	C_b/T
6-PBT	Hemispherical	FB	0.0002	0.1015	3.6	0.089
6-PBT	Hemispherical	FB	0.0002	0.1015	4.2	0.133
6-PBT	Hemispherical	FB	0.0002	0.1015	4.2	0.200
6-PBT	Hemispherical	FB	0.0002	0.1015	4.2	0.267
6-PBT	Hemispherical	FB	0.0002	0.1015	4.7	0.333
6-PBT	Hemispherical	UB	0.0002	0.1015	3.3	0.089
6-PBT	Hemispherical	UB	0.0002	0.1015	3.5	0.133
6-PBT	Hemispherical	UB	0.0002	0.1015	3.5	0.200
6-PBT	Hemispherical	UB	0.0002	0.1015	3.3	0.267
6-PBT	Hemispherical	UB	0.0002	0.1015	3.2	0.333
DT	Hemispherical	FB	0.0002	0.1025	3.5	0.200
DT	Hemispherical	FB	0.0002	0.1025	3.2	0.267
DT	Hemispherical	FB	0.0002	0.1025	3.4	0.333
DT	Hemispherical	UB	0.0002	0.1025	3.5	0.200
DT	Hemispherical	UB	0.0002	0.1025	3.7	0.267
DT	Hemispherical	UB	0.0002	0.1025	3.8	0.333
4-PBT	Torispherical	FB	0.0002	0.1906	3.9	0.089
4-PBT	Torispherical	FB	0.0002	0.1906	4.1	0.133
4-PBT	Torispherical	FB	0.0002	0.1906	4.3	0.200
4-PBT	Torispherical	FB	0.0002	0.1906	4.6	0.267
4-PBT	Torispherical	FB	0.0002	0.1906	4.8	0.333
4-PBT	Torispherical	PB	0.0002	0.1906	4.0	0.089
4-PBT	Torispherical	UB	0.0002	0.1906	4.3	0.089
4-PBT	Torispherical	UB	0.0002	0.1906	4.5	0.133
4-PBT	Torispherical	UB	0.0002	0.1906	4.6	0.200
4-PBT	Torispherical	UB	0.0002	0.1906	4.9	0.267
4-PBT	Torispherical	UB	0.0002	0.1906	5.6	0.333
RBI	Torispherical	FB	0.00015	0.2025	7.9	0.089
RBI	Torispherical	FB	0.00015	0.2025	10.3	0.133
RBI	Torispherical	FB	0.00015	0.2025	12.8	0.200
RBI	Torispherical	FB	0.00015	0.2025	12.8	0.267
RBI	Torispherical	FB	0.00015	0.2025	12.9	0.333
RBI	Torispherical	FB	0.0002	0.2025	8.8	0.089
RBI	Torispherical	FB	0.0002	0.2025	11.4	0.133
RBI	Torispherical	FB	0.0002	0.2025	13.3	0.200
RBI	Torispherical	FB	0.0002	0.2025	13.0	0.267
RBI	Torispherical	FB	0.0002	0.2025	13.4	0.333
RBI	Torispherical	PB	0.00015	0.2025	5.2	0.089
RBI	Torispherical	PB	0.0002	0.2025	6.1	0.089

Table A1 S-Value from Zwietering Equation (Continued)

Impeller Type	Type of Tank Bottom	Baffling Type	Particle Size, dp (m)	Impeller Diameter, D (m)	S-Value	C_b/T
RBI	Torispherical	UB	0.00015	0.2025	5.8	0.089
RBI	Torispherical	UB	0.00015	0.2025	6.2	0.133
RBI	Torispherical	UB	0.00015	0.2025	7.0	0.200
RBI	Torispherical	UB	0.00015	0.2025	6.1	0.267
RBI	Torispherical	UB	0.00015	0.2025	6.4	0.333
RBI	Torispherical	UB	0.0002	0.2025	6.2	0.089
RBI	Torispherical	UB	0.0002	0.2025	6.6	0.133
RBI	Torispherical	UB	0.0002	0.2025	6.8	0.200
RBI	Torispherical	UB	0.0002	0.2025	6.7	0.267
RBI	Torispherical	UB	0.0002	0.2025	6.9	0.333

REFERENCES

Armenante, P.M., Uehara-Nagamine, E., "Determination of correlations to predict the minimum agitation speed for complete solid suspension in agitated vessels." *Canadian Journal of Chemical Engineering,* **76,** pp. 413-419 (1998).

Brucato, A., Cipollina, A., "Particle suspension in top-covered unbaffled tanks." *Chemical Engineering Science* **65,** pp. 3001-3008 (2010).

Chomcharn, N., "Experimental investigation of mixing time in a stirred, torispherical-bottomed tank equipped with a retreat-blade impeller". M.Sc. Thesis, New Jersey Institute of Technology (2009).

Motamedvaziri, S., Armenante, P. M., "Flow regimes and surface air entrainment in partially filled stirred vessel for different fill ratios." *Chemical Engineering Science,* **81,**pp**.** 231-250 (2012).

Myers, K.J., Reeder, M.F., Fasano, J.B., "Optimize mixing by using the proper baffles." *CEP* (2002)

Scargiali, F., Busciglio, A., Grisafi, F., Tamburini, A., Micale, G., & Brucato, A., "Power consumption in uncovered unbaffled stirred tanks: influence of viscosity and flow regime." *Industrial & Engineering Chemical Research,* **52,** pp. 14998-15005 (2013).

Wijayasekara, D. B., "Minimum agitation speed for solid suspension and mixing time in a torispherical-bottomed pharmaceutical stirred tank under different baffling conditions." M. Sc. Thesis, New Jersey Institute of Technology (2010).

Zwietering, T. N. "Suspending solid particles in liquids by agitators." *Chem. Eng. Sci.* **8,** pp**.** 244-253 (1958).